LXR nuclear receptors are transcriptional regulators of dendritic cell chemotaxis

Susana Beceiro[1,#], Attila Pap[2#], Zsolt Czimmerer[2#], Tamer Sallam[3,4#], Jose A. Guillén[1], Germán Gallardo[1], Cynthia Hong[3], Noelia A-Gonzalez[1], Carlos Tabraue[1], Mercedes Diaz[1], Felix Lopez[1], Jonathan Matalonga[5], Annabel F. Valledor[5], Pilar Dominguez[6], Carlos Ardavin[6], Cristina Delgado-Martin[8], Santiago Partida-Sanchez[7], Jose Luis Rodriguez-Fernandez[8], Laszlo Nagy[2,9,10], Peter Tontonoz[3], and Antonio Castrillo[1]*

[1]Instituto de Investigaciones Biomédicas "Alberto Sols" CSIC-Universidad Autónoma de Madrid, Spain, Unidad de Biomedicina (Unidad Asociada al CSIC), Instituto Universitario de Investigaciones Biomédicas y Sanitarias (IUIBS), Grupo de Investigacion Medio Ambiente y Salud (GIMAS, ULPGC). Universidad de Las Palmas de Gran Canaria, Las Palmas, Spain.
[2]Department of Biochemistry and Molecular Biology, Faculty of Medicine, University of Debrecen, Debrecen, Hungary.
[3]Howard Hughes Medical Institute, Department of Pathology and Laboratory Medicine, University of California Los Angeles, California USA.
[4]Department of Medicine, Division of Cardiology, University of California, Los Angeles, California, USA.
[5]Departmento de Biología celular, Fisiología e Inmunología, Facultad de Biología, Universidad de Barcelona, Spain.
[6]Departamento de Inmunología y Oncología, Centro Nacional de Biotecnología, Consejo Superior de Investigaciones Científicas, Madrid, Spain.
[7]Center for Microbial Pathogenesis, The Research Institute at Nationwide Children's Hospital, Columbus, The Ohio State University, Columbus, Ohio, USA.
[8]Centro de Investigaciones Biológicas, Consejo Superior de Investigaciones Científicas, Madrid, Spain.
[9]MTA-DE “Lendület” Immunogenomics Research Group, University of Debrecen, Debrecen, Hungary.
[10]Sanford-Burnham-Prebys Medical Discovery Institute, 6400 Sanger Road, Orlando, FL, 32827, USA
[#] These authors contributed equally to this work

*CorrespondingAuthor:
Antonio Castrillo, Ph.D.
Instituto de Investigaciones Biomédicas "Alberto Sols" CSIC-Universidad Autónoma de Madrid, Spain and Unidad de Biomedicina (Unidad Asociada al CSIC), Instituto Universitario de Investigaciones Biomédicas y Sanitarias (IUIBS) de la Universidad de Las Palmas de Gran Canaria, Las Palmas, Spain.
Email: **acastrillo@iib.uam.es**

Running Title*: Liver X Receptors regulate DC migration*

Abstract

The liver X receptors (LXRs) are ligand-activated nuclear receptors with established roles in the maintenance of lipid homeostasis in multiple tissues. LXRs exert additional biological functions as negative regulators of inflammation, particularly in macrophages. However, the transcriptional responses controlled by LXRs in other myeloid cells, such as dendritic cells (DC), are still poorly understood. Here we used gain- and loss-of-function models to characterize the impact of LXR deficiency on DC activation programs. Our results identified an LXR-dependent pathway that is important for DC chemotaxis. LXR-deficient mature DCs are defective in stimulus-induced migration in vitro and in vivo. Mechanistically, we show that LXRs facilitate DC chemotactic signaling by regulating the expression of CD38, an ectoenzyme important for leukocyte trafficking. Pharmacological or genetic inactivation of CD38 activity abolished LXR-dependent induction of DC chemotaxis. Using the LDLR-/- mouse model of atherosclerosis, we also demonstrated that hematopoietic CD38 expression is important for the accumulation of lipid-laden myeloid cells in lesions, suggesting that CD38 is a key factor in leukocyte migration during atherogenesis. Collectively, our results demonstrate that LXRs are required for efficient emigration of DCs in response to chemotactic signals during inflammation.

Introduction

Dendritic cells (DCs) represent a heterogeneous population of professional antigen presenting cells (APCs) that arise from the bone marrow (BM) and reside in peripheral tissues and lymphoid organs (1, 2). DCs play central roles in initial recognition of pathogens and in the induction of antigen-specific adaptive immune responses. As sentinels located in peripheral tissues, immature DCs (iDCs) express a plethora of pattern recognition receptors and exhibit high endocytic capacity. Upon recognition and capture of microbial products, DCs undergo a maturation process, which is characterized by upregulation of co-stimulatory molecules and proinflammatory cytokines (3). Furthermore, mature DCs (mDCs) exhibit increased expression of the chemokine receptor CCR7, a G protein-coupled receptor critical for DC migration from peripheral tissues to lymphoid organs (4, 5). Thus, proper maturation and emigration of DCs from injured tissues are crucial for the initiation of antigen-dependent immune responses.

The liver X receptors (LXRα and LXRβ, encoded by *Nr1h3* and *Nr1h2* respectively), are ligand-activated transcription factors that belong to the nuclear receptor superfamily. LXRs function as key regulators of lipid homeostasis by controlling the expression of several genes that are pivotal for cholesterol, fatty acid and phospholipid metabolism (6-8). Both LXRs form obligate heterodimers with retinoid X receptors (RXRs) and positively regulate the expression of target genes through direct binding to promoter or enhancer regions containing specific sequences (DR4 elements or LXREs) (9). In addition to their role in lipid metabolism, LXRs also participate in the transcriptional regulation of inflammation and host defense (10-14). Ligand-activated LXRs are able to antagonize the expression of inflammatory genes in response to different insults, a process that has been extensively studied in macrophages (11, 13, 15).

Although the importance of LXRs in the immune system has received much attention in macrophages, transcriptional responses controlled by LXR in DCs are poorly understood relative to other lineages. In this study, applying LXR gain- and loss-of-function approaches, we define a novel contribution of LXR to DC gene expression programs that is important for DC chemotaxis. We show that the ability of LXRs to regulate DC migration in response to chemotactic signals is mainly accomplished via transcriptional regulation of CD38 expression. In addition, CD38 activity is important for the accumulation of lipid-laden myeloid cells in response to atherogenic inflammation. These results outline a previously unrecognized role for LXR signaling in the regulation of chemotactic responses in murine DCs through transcriptional induction of CD38 expression.

RESULTS

Contribution of LXRs during DC differentiation and maturation

Previous work has established that the transcriptional activity of LXRα and LXRβ in macrophages is important for the regulation of inflammation, phagocytosis and innate immune homeostasis (16). However, the impact of LXR signaling on DC function has not been explored in depth. We performed whole-genome microarray studies with RNA samples obtained from *in vitro* cultures of hematopoietic-derived human and mouse DCs (Figure 1 A-C). These experiments revealed that both LXRα and LXRβ were moderately to highly expressed in human and mouse DCs (Table 1). Furthermore, cluster analysis of nuclear receptor transcript levels revealed prominent expression of both LXRα and LXRβ in purified mouse and human tissue DC populations (Figure 1C). These experiments also revealed that bone marrow-derived DCs (BMDCs) and splenic or lymph node classic DCs express higher transcript levels of LXRα when compared to LXRβ (Figure 1C). Public repositories of transcript datasets show expression levels of LXR subtypes in DCs that are consistent with our observations (17).

To investigate the impact of endogenous LXR activity on DC differentiation and maturation *in vitro*, we employed flow cytometry to assess the expression of classic DC activation markers in cultured monocyte-derived DCs (MoDCs) obtained from WT and LXR-deficient (lacking both *Lxrα* and *Lxrβ* genes; designated here as LXR-DKO) mice. Activation of MoDCs with the TLR4 agonist LPS increased expression of CD11c and of co-stimulatory molecules required for T-cell priming, including major histocompatibility complex class II (MHC-II), CD80, CD86 and CD69, in both WT and LXR-DKO MoDCs (Figure 2A-B). To validate these results *in vivo*, spleen and LN classic MHC-II^{hi}/CD11c^{hi} DCs (that express high levels of LXRs in WT mice) were present at similar frequency in samples obtained from WT and LXR-DKO mice (Figure 2C). We also identified DCs by histological examination of spleen and lymph node cryosections immunolabeled with a CD11c antibody. Analysis of WT and LXR-DKO samples

showed similar distribution of DCs in both tissues, with CD11c+ cells localized primarily within the T-cell zone (Figure 2C). Consistent with these results, analysis of MHC-II+ cells obtained from ear epidermal sheets did not reveal appreciable differences in the expression of the myeloid markers CD68 or Langerin in samples from WT and LXR-DKO mice (Figure 2D and data not shown). Together, these data suggest that endogenous LXR activity is not required for the development or differentiation of DCs *in vitro* or *in vivo*.

We next investigated whether *in vitro* maturation of DCs promoted changes in established LXR target genes in cultured MoDCs. (Figure 3A) (18-20). We observed that DC maturation induced by LPS led to the upregulation of some LXR targets and to the downregulation of others (Figure 3A-B). These results indicate that LXR-dependent gene expression in DCs might be influenced by various factors, such as endogenous LXR ligand availability. Furthermore, although LXR activity has been studied in mature DCs with pharmacological activation approaches using synthetic agonists *in vitro* (17, 18, 21), we considered the possibility that additional LXR target genes important for DC immune functions might arise using our LXR genetic loss-of function system.

To study the influence of endogenous LXR signaling on DC gene expression programs in depth, we conducted global gene expression analysis in WT and LXR-DKO DCs stimulated 24h with LPS. Using a stringent cut-off threshold of 5-fold or higher, we concentrated on the subsets of genes that were highly induced by DC maturation. In agreement with published studies (22), a considerable proportion of genes whose expression was induced by LPS in both WT and LXR-null cells were known targets with direct functions in antimicrobial and inflammatory responses in DCs (Figure 3C). Interestingly, the magnitude of changes in inflammatory gene expression during DC maturation was generally higher in LXR-DKO cells when compared to WT control DCs (Figure 3C central heat map). These results are consistent with the anti-inflammatory role of LXRs in other cell types (15). In addition, LXR-DKO cells presented a substantial increase in the number of maturation-induced genes, likely reflecting the existence of several de-repressed inflammatory pathways in the absence of LXR.

Identification of LXR-regulated genes during DC maturation

In an effort to identify LXR-regulated genes in DCs that might contribute to LXR functions in immunity, we analyzed a subgroup of genes whose expression was preferentially *up*-regulated in WT but not in LXR-DKO cells during DC maturation. We identified a set of genes (<30) whose expression was differentially induced in WT mature DCs (Figure 2C). The gene set included those encoding proteins with previously defined roles in innate immunity, inflammation and chemotaxis, such as the interferon-responsive IFIT2 and GBP3, the chemokine CXCL16 and the ectoenzyme CD38 (Figure 2C and supplementary Table 2). DC maturation with LPS also promoted the expression of the established LXR target *Abca1*, in an LXR-dependent manner (Figure 4A).

We further tested whether the expression of genes in this maturation-dependent cluster was acutely responsive to activation of LXR/RXR heterodimers by synthetic ligands. *Abca1* expression was potently induced upon LXR activation as expected. Interestingly, within this cluster of maturation-dependent genes, we found that mRNA levels of *Cd38* were consistently up-regulated by synthetic LXR ligand GW3965 in WT DCs but not in LXR-DKO cells (Figure 4B). In addition, induction of *Cd38* expression by LXRs was more prominent in mature DCs when compared to immature DCs (Figure 4B).

The gene encoding the ectoenzyme CD38 has been recently identified as an LXR target in macrophages in a separate report by some of the authors of the present manuscript (14). Since Matalonga et al. evaluated LXR-dependent regulation of CD38 expression in the context of macrophage anti-bacterial responses, we decided to further study the impact of LXR-CD38 signaling in DCs in more detail. CD38 is a type-II transmembrane glycoprotein highly expressed by hematopoietic and non-hematopoietic cells. Also known as adenosine-5′-diphosphate-ribosyl cyclase 1, CD38 is a multifunctional enzyme that presents both extracellular and intracellular activities, including the ability to produce cyclic

adenosine diphosphoribose (cADPR) and ADP-ribose (ADPR) from nicotinamide adenine dinucleotide (NAD+). Interestingly, CD38 actions have previously been linked to leukocyte trafficking in response to inflammation, and *Cd38*-/- mice mount inefficient innate and adaptive immune responses (23, 24). The experiments above indicated that CD38 expression is transcriptionally regulated by LXRs in murine DCs. Further analysis revealed that CD38 protein expression (analized by immunocytochemistry and flow cytometry) was severely compromised in mature LXR-DKO DCs in comparison to WT cells (Figure 4C-D). Moreover, *Cd38* mRNA expression was also induced in response to LXR agonists in human monocyte-derived DCs (Figure 5), suggesting that the regulation of CD38 expression by LXRs is preserved across species.

LXR is required for efficient CCR7-dependent chemotaxis in DCs

Previous work demonstrated that CD38 is important for host responses against pathogens, including *L. monocytogenes, S. pneumonia* and *S. typhimurium* (14, 23, 24). Further studies concluded that migratory defects in bone-marrow derived cells underlie the increased susceptibility to infection in *Cd38*-/- mice. We therefore considered the possibility that LXR signaling might be contributing to chemotactic activity in DCs by regulating CD38 expression. To test this hypothesis, we used migration assays to analyze the chemotactic capacity of WT and LXR-DKO DCs in response to CCL21 and CCL19, which are ligands of the G protein–coupled receptor CCR7. Importantly, equivalent mRNA and protein levels of CCR7 were observed in WT and LXR-DKO DCs in response to TLR-activation signaling (Figure 6A and data not shown). It is well documented that immature DCs present weak migratory capacity in response to CCL21 and CCL19 (25, 26). Consistent with these studies, both WT and LXR-DKO immature DCs did not respond significantly to CCL19 and CCL21 stimulation (Figure 6B left panel). Remarkably, while mature WT DCs migrate robustly towards CCL21 or CCL19 grandients, a drastic decrease in chemotactic activity to both ligands was observed in LXR-DKO DCs (Figure 6B right panel).

To further characterize the impact of LXR activity on DC migration, primary splenic DCs that had been pretreated with vehicle or GW3965 were analyzed in transwell migration assays in response to CCR7 ligands. Activation of LXRs by GW3965 potentiated CCL19- and CCL21-dependent migration of mature wild-type but not LXR-DKO DCs (Figure 6C). These results indicate that while CCR7 expression is comparable in primary WT and LXR-DKO DCs, chemokine-induced migration is significantly regulated by LXR expression and activity in murine DCs.

In addition to promoting chemotaxis, activation of CCR7 affects several additional functions of mature DCs, including survival (27, 28). These functions have been shown to be regulated by distinct downstream signaling pathways (29). While CCR7-dependent survival of DCs is mainly regulated by PI3K/Akt signaling, DC chemotaxis is controlled by MAPK signalling. Since both LXR and CD38 regulate DC chemotaxis, we considered whether LXR-CD38 axis may participate in chemotactic signaling by regulating MAPK pathways downstream of CCR7. Stimulation of WT DCs with CCL19 resulted in a rapid activation of ERK1/2 and Akt as expected (30, 31) (Figure 6D). In contrast, CCL19-induced phosphorylation of ERK1/2 was markedly inhibited in LXR-DKO DCs. Interestingly, the level of Akt activation in response to CCL19 stimulation was similar in WT and LXR-DKO cells. These results indicate that LXR activity is important for chemokine-induced activation of intracellular pathways that direct migration of DCs, but is dispensable for CCR7-dependent survival pathways.

DC migration *in vivo* is impaired in LXR-deficient mice

To investigate whether LXRs play a role in DC migration *in vivo*, we employed two widely accepted models. First, we used the classic approach of FITC skin painting to monitor the migration of endogenous skin antigen-presenting cells (26). Epicutaneous application of FITC under inflammatory conditions stimulates the activation and migration of DCs carrying FITC antigen to draining lymph nodes. Immunofluorescence analysis of LNs obtained from FITC-painted mice showed that LXR-DKO LNs contained few CD11c+/FITC+ DCs when compared to WT LNs (Figure 7A, left panel). Consistent with this

result, flow cytometry analysis of LN cell suspensions revealed decreased number of migrated FITC+ DCs 24-48 h after FITC-painting in LXR-DKO versus WT mice (Figure 7A, bottom panel). Thus, LXR signaling is important to guide the migration of endogenous DCs to LNs in response to an antigenic stimulus *in vivo*.

To determine whether the migration deficit observed in LXR-DKO DCs was cell intrinsic, we used a second model in which we co-injected differentially-labelled activated DCs from WT and LXR-DKO mice into footpads of recipient mice. Draining LNs were collected 24 h post injection, and the presence of migrated DCs was assessed by flow cytometry and immunofluorescence microscopy. While WT DCs reached the draining LN after subcutaneous injection, a consistent decrease in the frequency of LXR-DKO DCs was detected by both experimental approaches (Figure 7B). These results confirm that LXR-DKO DCs have impaired migratory capacity *in vivo* due to a cell-intrinsic defect.

CD38 is required for LXR-dependent DC chemotaxis

Although CD38 catalyzes the production of several nucleotide-based metabolites from NAD(P)+, the generation of cADPR has been shown to be particularly relevant for the immunoregulatory functions of CD38 (32). Previous studies using the cADPR antagonist 8Br-cADPR demonstrated that CD38 regulates calcium flux and migration of chemokine-activated DCs in a cADPR-dependent manner (33). To determine the impact of CD38 catalytic activity on LXR-dependent DC chemotaxis, we analysed the migration responses of WT and LXR-DKO DCs that were pre-treated with GW3965 in the presence or absence of 8-Br-cADPR. Chemotaxis in response to CCL19 was greatly reduced in cells cultured with 8-Br-cADPR, in agreement with previous reports (Figure 8A). Interestingly, inhibition of CD38 enzymatic product activity by 8-Br-cADPR blocked GW3965-dependent induction of chemotaxis in wild-type DCs, but had little effect on LXR-DKO cells (Figure 8A). These results indicate that ligand-activated LXRs contribute to the regulation of DC chemotaxis through the generation of CD38-dependent enzymatic products.

To definitely assess the importance of LXR-CD38 signaling in the

283 regulation of DC chemotaxis, we used a CD38 genetic loss of function model. As
284 shown in figure 8B, stimulation of CCR7-dependent DC chemotaxis by LXR
285 ligand was abolished in *Cd38*-/- cells, indicating that LXR-dependent induction of
286 *Cd38* expression is functionally relevant during DC activation and migration.
287 Interestingly, LXR-deficient DCs showed decreased chemotaxis capacity
288 compared to *Cd38*-/- cells (Figure 8B), suggesting that LXR signaling participates
289 in DC migration pathways through both CD38-dependent and independent
290 mechanisms.
291 We also analyzed the impact of CD38 deficiency on the frequency of
292 circulating leukocytes under homeostatic conditions or in response a regimen of
293 bone marrow transplantation. Blood count comparisons indicate that CD38
294 activity does not affect substantially the number of circulating myeloid/lymphoid
295 populations under homeostatic conditions or after transplantation of bone marrow
296 precursors (figure 9A). Furthermore, we analyzed the frequency of CD11c+ cells
297 in spleen, bone marrow and skin of irradiated WT mice (CD45.1) reconstituted
298 with WT or CD38-/- (both CD45.2) progenitors. WT and CD38-/- donor-derived
299 CD11c+ cells were present in spleen, bone marrow and skin of transplanted mice
300 with similar efficacy. Interestingly, within this fraction of CD11c+ transplanted skin
301 cells, however, CD38-/- DCs responded inefficiently to an inflammatory challenge
302 in the skin (figure 9D), further supporting the idea that CD38 is required to
303 effective chemotaxis in response to inflammation.
304
305 **CD38 activity in hematopoietic cells affects atherosclerosis development.**
306 LXR-dependent gene expression in bone marrow-derived myeloid cells
307 has been shown to impact the development of atherosclerosis through various
308 mechanisms (34). We hypothesized that the regulation of *cd38* expression by
309 LXRs in myeloid cells may contribute to the migratory capacity of phagocytic cells
310 during atherosclerosis. To test this idea, we transplanted bone-marrow progenitor
311 cells obtained from WT or *Cd38*-/- mice into lethally irradiated *Ldlr*-/- mice and
312 analyzed lesion formation after a regimen of western diet feeding. We confirmed
313 efficient bone-marrow engraftment after transplant by analyzing *Cd38* mRNA

expression (not shown). We did not observe changes in body weight or plasma cholesterol levels between *Cd38*-/- and WT reconstituted mice (not shown). Remarkably, however, quantification of atherosclerosis by *en face* analysis after 18 weeks of diet revealed a significant reduction in atherosclerotic burden in *Ldlr*-/- recipients reconstituted with *Cd38*-/- bone marrow compared to WT reconstituted *Ldlr*-/- mice (Figure 10A. N=15-20 mice per group). Immunohistochemical analysis using CD68 antibody revealed a considerable reduction of total macrophage infiltration within lesions of *Cd38*-/- transplanted mice (Figure 10B-C). Analysis of the relative signal of CD68 antigen per atherosclerotic lesion denoted a trend towards the same tendency; however, it did not reach statistical significance (Figure 10D). Overall, these results indicate that CD38 activity in myeloid cells is determinant of atherosclerosis susceptibility and further suggest that CD38-dependent chemotaxis mechanisms play an important role in the infiltration of mononuclear cells during early atherosclerosis development. Collectively, our results outline a novel pathway by which LXRs participate in myeloid-derived DC migration through direct regulation of CD38 expression.

DISCUSSION

LXRs are crucial regulators of lipid metabolism that exert important functions in inflammation and host immunity (12, 15, 34, 35). Although the LXR pathway has been extensively studied in macrophages under inflammatory conditions, little is known about LXR transcriptional programs in DCs. Indeed, to our knowledge, this work is the first to report LXR actions in DCs using complete genetic LXR deficiency (both LXRα and LXRβ double deficiency) *in vitro* and *in vivo.* We present a comprehensive analysis of LXR transcriptional activity in primary DCs combining pharmacological and genetic manipulation of the LXR pathway with global gene expression analysis in models of DC activation. Our results revealed that LXR activity potentiates DC chemotaxis *in vitro* and *in vivo*. We further showed a plausible mechanism by which LXRs modulate DC chemotaxis through transcriptional regulation of CD38 expression.

Immune responses are initiated in secondary lymphoid organs, where DCs migrate to present antigens to naive T and B cells (2). The ability of DCs to migrate requires the expression of the lymphoid homing receptor CCR7 by maturing DCs (4). Using two *in vivo* models of stimulus-induced chemotaxis, we demonstrated that migration of DCs to draining lymph nodes requires an intact LXR signaling pathway. It is possible that if lymphocytes encounter reduced numbers of antigen-presenting cells due to impaired chemotaxis, the development of an acquired immune response might be compromised in LXR deficient mice. Although *in vivo* adaptive immunity has not been addressed in depth in LXR-null mice, these mice present abnormal lymphocyte proliferation and develop autoimmunity with age (36, 37). Therefore, additional studies will be required to determine the role of LXR-dependent migration of APCs in the context of adaptive immunity. For example, through the generation of new mouse models of LXR conditional deletion in APCs, it should be possible to directly test the contribution of LXR-dependent DC migration in the context of adaptive immunity.

In view of the impaired migratory capacity of LXR-DKO DCs, we examined the level of activation of chemokine-dependent signaling pathways in our DC culture system. Our findings revealed that, although the magnitude of intracellular Akt activation was equivalent, induction of the MAPK pathway by chemokines was defective in LXR-DKO DCs compared to WT cells. Previous studies reported that pharmacological LXR activation can influence, both positively and negatively, the expression of the chemokine receptor CCR7 in different cultured cells *in vitro* or *in vivo* in models of disease, such as atherosclerosis regression or tumor progression (38-41). The reasons for these contrasting results are not entirely clear, but could be due to differences in basal CCR7 expression levels that may not be similarly regulated upon stimulation among the particular models of cellular activation. Alternatively, the employment of different doses of various activating agonists, either synthetic ligands or natural oxysterols, under different culture conditions may account for these contrasting results (38-41). Nevertheless, our results using genetic LXR deficiency indicate that primary LXR-null DCs express equivalent CCR7 levels compared to WT cells during DC maturation. Thus, deficiency of LXR renders DCs hyporesponsive to CCL19/CCL21 chemokines, despite normal expression of CCR7 and several other maturation markers. Importantly, maturation of DCs promoted the expression of several LXR targets, including *Abca1* and *Cd38*, while inhibiting others such as *Srebf1*. Interestingly, although LXR is not the sole transcription factor involved in the expression of those targets, upregulation of *Abca1* and *Cd38* by mature DCs was found to be largely dependent on LXR expression. This suggests that endogenous LXR activators might be generated during DC maturation by inflammatory signals. Alternatively, given that other LXR targets were down-regulated by DC maturation, an integrative view points to gene-specific epigenomic changes in which LXR and/or coregulator binding at target locations might be modified by inflammation. Further work will be required to delineate the specific genomic locations of LXR during inflammatory activation of DCs.

Using models of LXR pharmacological activation and LXR deficiency in DCs, we showed that LXRs directly upregulate CD38 expression in primary DCs. CD38 is a multifunctional enzyme that belongs to the ADP-ribosylcyclase family and has both ectoenzyme and receptor functions. Previous studies demonstrated that CD38-deficient mice are unable to mount an effective immune response against bacterial infections (14, 23, 24). The inability of myeloid cells to directionally migrate to sites of infection was reported to be a possible explanation for the defective anti-microbial responses in those mice. Interestingly, both LXR and CD38 deficient mice present immune defects against bacterial infections (12, 14, 23, 42). Because LXR regulates the expression of CD38, the migration of specific subsets of APCs *in vivo* to sites of infection in the context of LXR-deficiency could be an interesting angle to explore in future studies. However, such studies could be also confounded by the fact that LXR-null mice are defective in splenic marginal zone macrophages (35), a specific subset of macrophages important for the systemic capture of circulating antigens. Thus, new mouse models with APC-specific deficiency of LXR in which splenic marginal zone was not affected would be potentially eligible for the analysis of recruitment of APCs in response to systemic infections.

Importantly, other studies have documented the cellular localization of CD38 in lipid-rich membrane domains. Association of CD38 with membrane signaling receptors, including CCR7, CD83 and CD11b, has been reported in human Mo-DCs (43). Since CD38 ensures efficient migration in response to CCR7 ligands (32, 44), it is therefore possible that ligation of CCR7 induces interactions with CD38 and other signaling receptors within lipid rafts in which membrane cholesterol fluidity is important (45). Thus, cooperation between CCR7, CD38 and perhaps other receptors in lipid rafts may regulate innate and adaptive immune responses by modulating DC migration and survival. We found that the influence of LXR signaling on this DC chemokine signaling crosstalk was largely dependent on CD38 expression. Loss of CD38 abolished LXR-dependent

induction of CCR7-dependent chemotaxis. Interestingly, LXR-deficient DCs presented a more profound impairment in DC chemotaxis compared to CD38-/- DCs, suggesting that LXR signaling participates in multiple pathways that control DC chemotaxis, both CD38 dependent and independent. One possibility is that accumulation of excess cholesterol in membrane microdomains in LXR-DKO DCs could be altering the interaction between chemokine receptors and co-receptors important for migration signaling.

Migration of myeloid cells into the artery wall in response to chemotactic molecules is one of the key steps in early atherosclerotic lesion formation (46). In this regard, although recruitment of monocytes may initially serve as a protective mechanism to remove excess LDL cholesterol and reduce inflammation, progressive accumulation of cells in the artery wall in the context of hypercholesterolemia ultimately leads to atheroma formation. Many studies have demonstrated that interference with myeloid chemotaxis retards the development of atherosclerosis (47). On the other hand, in surgical models of plaque regression, in which aortas of hypercholesterolemic mice are transplanted into WT mice, reduction of cholesterol loading in lesional myeloid cells has been shown to induce their emigration from plaques and alleviate atherosclerosis (48). Atherosclerosis regression in these models was shown to be impaired in the absence of LXRα or LXRβ and associated with decreased CCR7 expression in myeloid cells (38). Accordingly, CCR7-dependent chemotaxis of myeloid cells back to draining lymph nodes appears to play a beneficial role in the context of regression of atherosclerosis in surgical models. However, other studies have implicated CCR7 expression and CCL19/CCL21 ligands in the progression of atherosclerosis (49, 50). Thus, the migratory capacity of myeloid cells has been associated with both attenuation and exacerbation of atherosclerosis in different models.

Although studies with knockout mice of some individual LXR target genes have shown divergent effects in atherosclerosis, the net result of LXR activation

469 is clearly atheroprotective (34). This is due to the fact that LXRs regulate the
470 expression of a number of genes whose activity promotes removal of cholesterol
471 from plaque myeloid-derived foam cells. We showed that the connection between
472 CD38 and DC migration has pathophysiological relevance in the LDLR-/- model
473 of atherosclerosis. Loss of hematopoietic CD38 expression alleviates atherogenic
474 lesion progression. Defective chemotactic capacity of CD38-/- myeloid cells is
475 likely a contributing factor to this phenotype. These observations suggest that
476 novel CD38 inhibitors could have therapeutic benefit in the setting of
477 atherosclerosis
478 Collectively, our results uncover a previously-unrecognized mechanism that
479 operates in DCs in which LXRs modulate chemokine signaling in mature DCs, at
480 least in part, through the potentiation of CD38 expression.

Material and methods

Animals

LXR-deficient (*Nhr1h3-/-Nhr1h2-/-*) (LXR-DKO) mice on a mixed Sv129/C57BL/6 were originally provided by David Mangelsdorf (UTSW)(51) and CD38-deficient mice (N-B6.129P2-Cd38 tm1Lnd) had been backcrossed to C57BL/6 background for more than ten generations. All mice were maintained under pathogen-free conditions in a temperature-controlled room and a 12-hour light-dark cycle in the animal facilities of ULPGC and NCH/OSU. All animal studies were conducted in accordance with institutional participants' animal ethics research committees. WT and CD38 deficient mice (N=5 each group) were euthanized and blood was collected from cardiac puncture and stored in EDTA coated tubes. Leukocyte counts were determined using an Abacus JuniorVet (Diatron®) hematologic counter.

Reagents

Recombinant murine CCL19, CCL21 and granulocyte-macrophage colony-stimulating factor (GM-CSF) were from Peprotech (London, United Kingdom). The synthetic LXR ligand GW3965 was provided by J. Collins (Glaxo SmithKline). LPS Serotype 055:B5 and 8-Br-cADPR were from Sigma. CellTracker Green (CMFDA) and CellTracker Red (CMTPX) were obtained from Molecular Probes.

Cell isolation and culture

Monocyte-derived DCs (MoDCs) were prepared as described(52). In brief, bone marrow (BM) monocytes were purified from cell suspensions through depletion of T cells, B cells, granulocytes, NK cells and DCs with antibodies that recognize B220, MHC-II, Thy1.2, CD43 and CD24. Averages of 90-95% of monocytes were collected from negatively selected cells. MoDCs were obtained by culturing monocytes with GM-CSF for 24 hours. In other set of experiments, BM-derived DCs (BMDCs) were generated *in vitro* as described(53) with modifications. BM cells were cultured for 6-7 days in RPMI 1640 medium containing 10% fetal

bovine serum (FBS) supplemented with mouse GM-CSF (20 ηg/mL) every two days. Non-adherent cells were collected and further enriched in DCs by positive selection with CD11c microbeads (MiltenyiBiotec). For isolation of DCs from lymphoid tissues, spleen or lymph nodes were digested with 1 mg/mL Liberase CI (Roche), 40 mg/mL DNAse I (Roche) and 1% (vol/vol) FBS, for 30 minutes at 37°C in RPMI medium. Cell suspensions were enriched by positive selection with CD11c microbeads (Miltenyi Biotech) and further purified by FACS sorting using CD11c and MHC-II antibodies. The purity of the DC population based on CD11c and MHC-II expression was >90% by flow cytometry analysis. For DC activation, MoDCs, BMDCs or purified DCs from lymphoid tissues cells were stimulated with LPS (10 ng/mL, *E. coli*, Sigma-Aldrich) for 24h.

Flow cytometry

Single-cell suspensions (1×10^6 cells) were washed twice in staining buffer (PBS with 0.1% BSA and 0.1% sodium azide), and incubated with Fc-block (anti-CD16/32, Sigma-Aldrich) for 20 minutes at 4°C. Cells were incubated with labeled antibodies for 30 minutes at 4°C. Intracellular CCR7 staining was performed following commercial instructions (eBioscience). Cells were then analyzed on BD FACSCalibur or FACSCanto II (Becton Dickinson) with FlowJo software (TreeStar, Inc.). Detailed description of antibodies used for flow cytometry is listed in supplementary table 1.

RNA and protein analysis

Total RNA was obtained with TRIzol reagent (Invitrogen). RNA was reverse-transcribed with iScript reverse-transcription kit (Bio-Rad). Real-time quantitative PCR (qPCR) was performed with a Bio-Rad iQ5 detector and SYBR green assays as described previously(35). Expression was normalized to 36B4 expression. Primer and probe sequences are listed as supplementary material.

For western blot analysis, DCs were stimulated with CCL19 for the indicated times. The stimulation was terminated by solubilizing the cells in 100 µL ice-cold RIPA buffer supplemented with protease and phosphatase inhibitor (Sigma).

Lysates were resolved by SDS-PAGE and transferred to nitrocellulose (Bio-Rad Laboratories) membranes. Membranes were incubated with the indicated antibodies (Supplementary Table 1). Blots were washed and visualized with the appropriate horseradish peroxidase (HRP)–conjugated secondary antibodies (Bio-Rad), and ECL kit (ECL-Plus, Amersham Biosciences) and Bio-Rad Chemi-Doc imaging system. Detailed description of antibodies used for is listed in supplementary table 1.

Histology and immunofluorescence staining

Lymph nodes and spleens were embedded in OCT compound (Tissue-Tek), and snap-frozen in dry-ice and isopentane. 4-8 μm frozen sections were air-dried, fixed with 4% paraformaldehyde, blocked with 6% BSA and 2% preimmune serum in PBS, and stained with fluorescence-conjugated antibodies diluted in blocking solution.

***In vitro* migration assay**

In vitro chemotaxis assays were performed using migration chambers. Briefly, DCs were cultured in Transwell chambers (5-μm pore size, Costar) with 100 ng/mL of CCL19 and CCL21 or control solvent at the lower chamber. After 3 hours of incubation at 37°C, migrated cells were quantified using an automated cell counter (TC-20 Biorad). When indicated, cells were pretreated for 30 minutes with 8Br-cADPR (10 μM) or with GW3965 (1 μM) for 18 hours. Each experiment was performed in triplicate. The results are expressed as the mean ± SD of the chemotactic index (CI) for triplicate wells. The CI represents the fold increase in the number of migrated cells in response to chemoattractants over the spontaneous cell migration in response to control medium conditions.

***In vivo* DC migration assays**

Mouse abdominal and inguinal areas were gently shaved. Fluorescein isothiocyanate (FITC, 0,5%) was dissolved in acetone:dibutylphthalate (1:1), and applied to mouse exposed area(54). After 24-48 hours, draining inguinal LNs

were harvested and processed. To test *in vivo* migration of *ex vivo* differentiated cells, WT and LXR-deficient mature BMDCs were labeled with 1 μM of CellTracker Green CMFDA or CellTracker Red CMTPX, respectively and resuspended in PBS. $1x10^6$ DCs at a 1:1 ratio were injected subcutaneously into the hind footpads of control mice (55). 24 hours later after injection, popliteal LNs were harvested. Representative LN samples from each mouse were processed for immunofluorescence analysis or flow cytometry.

Microarray Analysis

Total RNA was isolated from iDCs and mDCs (stimulated with LPS 100 ng/mL for 24h) BMDCs using RNeasy kit (Qiagen) according to manufacturer's protocol. RNA quality was assessed on Agilent Bioanalyzer 2100 (Agilent Technologies). Transcriptional profiling were performed as follows: mouse Affymetrix 430 2.0 microarrays at the Genomics core facility, Universidad Complutense, Parque Científico de Madrid, Spain and at the Center for Clinical Genomics and Personalized Medicine Microarray Facility (University of Debrecen, Hungary). Affymetrix Gene Chip Human Genome U133 Plus 2.0 were conducted at the Microarray Core Facility of European Molecular Biology Laboratory (Heidelberg, Germany). Data were analyzed with GeneSpring and GeneChip Analysis Suite software (Affymetrix) as described previously[57]. Only statistically significant expression differences are presented. Raw signal intensities were normalized per chip (to 50th percentile). We removed probe sets that failed to reach a raw signal intensity of 50 (human monocyte-derived DCs) and 75 (mouse BMDCs) in all three samples. These values represented roughly the median of the signal intensity values of all probe sets. We defined the remaining probe sets as expressing genes. Next, we calculated the median of raw values of expressing genes and created two categories. Highly expressed genes involved the expressed genes with raw values over median, while expressed genes with raw values under median were in moderately expressed gene category. All datasets are available through the GEO NCBI server or ArrayExpress database. Accesion numbers are: GSE109277 and GSE109284 (this manuscript), GSE15907 (public

dataset from IMMGEN consortium), GSE23618 (human DC data) and E-TABM-34 (ArrayExpress database DC subsets in human tonsils and blood).

Isolation and culture of human DCs and mouse epidermal sheets

Human peripheral blood mononuclear cells (PBMCs) were isolated from healthy volunteer's buffy coats over by Lymphoprep (NycomedPharma, Oslo, Norway) gradient centrifugation according to standard procedures, followed by immunomagnetic separation with anti-CD14-conjugated MicroBeads (VarioMACS separation System, Miltenyi Biotec). Monocytes were cultured in 6-well plates at a density of 10^6 cells/ml in RPMI 1640 medium (Sigma-Aldrich) supplemented with 10% FBS (Invitrogen), 2mM L-glutamine (Invitrogen) and penicillin/streptomycin (Sigma-Aldrich). For DC differentiation we treated the freshly isolated monocytes with 800 U/ml GM-CSF (Leucomax, Gentaur Molecular Products) and 100 ng/ml IL-4 (PeproTech) for 5 days. Epidermal sheets were obtained from ears of wild-type and LXR-deficient mice as described earlier [4] . Briefly, ears were split into dorsal and ventral halves and floated split side down for 2 hours on 20 mM EDTA in PBS at 37°C. The epidermis was separated from the dermis with fine forceps, washed twice in PBS and fixed in ice-cold acetone for 20 minutes at room temperature. After rehydration in PBS, sheets were processed as described previously for lymph nodes and spleen. To detect the cell nucleus, samples were stained with 4',6-diamidino-2-phenylindole (DAPI; Sigma-Aldrich). Sections were observed with an LSM 5 PASCAL laser-scanning microscope (Carl Zeiss).

Bone marrow transplant histological and lesion analysis

Recipient male LDLR−/− mice (Jackson Laboratory B6.129S7-*Ldlrtm1Her*/J) or WT C57Bl6 CD45.1 were lethally irradiated with 900 rads and transplanted with $3x10^6$ BM cells from 8 week or older donors (WT or CD38) via tail vein injection as previously described (56). After four weeks of recovery, LDLR-/- transplanted mice were fed Western Diet (Research Diets D12079B) for 18 weeks. Mice were euthanized and perfused with 0.5mM EDTA/PBS. Aortas were dissected, fixed

(4% paraformaldehyde, 5% sucrose, 20 μM/EDTA), pinned, and stained with Sudan IV. Images were captured with a CCD camera. Atherosclerosis in the aortic roots and the descending aortas (*en face*) were quantified by computer-assisted image analysis as described (57, 58). Lesion development is expressed as the percentage of total aortic surface covered by lesions (57). The preparation and staining of frozen sections from aortas were performed as described previously. The following antibodies were used for immunohistochemistry: CD68 (MCA1957GA, AbD) 1:400 with secondary antibody biotin-SP-conjugated AffiniPure goat anti-rat IgG (H+L) (Jackson Laboratories).

Statistical analysis

Experimental groups include at least 4/5 mice. All experiments were performed at least 3 times. Data were expressed as mean ± SD. Statistical analyses were performed with SPSS software (IBM). An ANOVA-Bonferroni test or a Student's T-test were used to determine statistical differences between multiple or paired comparisons with normal distribution of the data.

Acknowledgments

We thank David Mangelsdorf (University of Texas Southwestern) for the LXR null mice, Jon Collins (GlaxoSmithKline SA North Carolina) for the LXR agonist GW3965 and Andres Hidalgo and Lisardo Bosca for reagents and comments; This work was supported by the following grants: Spanish Ministry of I+D SAF2008-00057, MINECO SAF2011-29244, SAF2014-56819-R, Comunidad de Madrid I+D Grant S2010/BMD-2350 to A.C, SAF2014-57856 to A.F.V, the NuRCaMeIn network (SAF2015-71878-REDT to A.F.V and AC), NIH HL-066088 and HL-030568 to P.T. SB was supported in part by a fellowship from Spanish Ministry of I+D BES2006-12056 and J.M. received a fellowship from the Spanish MICINN (FPI, BES-2009-014828).

REFERENCES

1. Steinman RM. 1991. The dendritic cell system and its role in immunogenicity. *Annu Rev Immunol* 9: 271-96
2. Banchereau J, Steinman RM. 1998. Dendritic cells and the control of immunity. *Nature* 392: 245-52
3. Satpathy AT, Wu X, Albring JC, Murphy KM. 2013. Re(de)fining the dendritic cell lineage. *Nat Immunol* 13: 1145-54
4. Ohl L, Mohaupt M, Czeloth N, Hintzen G, Kiafard Z, Zwirner J, Blankenstein T, Henning G, Forster R. 2004. CCR7 governs skin dendritic cell migration under inflammatory and steady-state conditions. *Immunity* 21: 279-88
5. Forster R, Davalos-Misslitz AC, Rot A. 2008. CCR7 and its ligands: balancing immunity and tolerance. *Nat Rev Immunol* 8: 362-71
6. Venkateswaran A, Laffitte BA, Joseph SB, Mak PA, Wilpitz DC, Edwards PA, Tontonoz P. 2000. Control of cellular cholesterol efflux by the nuclear oxysterol receptor LXR alpha. *Proc Natl Acad Sci U S A* 97: 12097-102
7. Schultz JR, Tu H, Luk A, Repa JJ, Medina JC, Li L, Schwendner S, Wang S, Thoolen M, Mangelsdorf DJ, Lustig KD, Shan B. 2000. Role of LXRs in control of lipogenesis. *Genes Dev* 14: 2831-8.
8. Hong C, Tontonoz P. 2014. Liver X receptors in lipid metabolism: opportunities for drug discovery. *Nat Rev Drug Discov* 13: 433-44
9. Tontonoz P. 2011. Transcriptional and posttranscriptional control of cholesterol homeostasis by liver X receptors. *Cold Spring Harb Symp Quant Biol* 76: 129-37
10. Castrillo A, Joseph SB, Marathe C, Mangelsdorf DJ, Tontonoz P. 2003. Liver X receptor-dependent repression of matrix metalloproteinase-9 expression in macrophages. *J Biol Chem* 278: 10443-9
11. Glass CK, Saijo K. 2010. Nuclear receptor transrepression pathways that regulate inflammation in macrophages and T cells. *Nat Rev Immunol* 10: 365-76
12. Joseph SB, Bradley MN, Castrillo A, Bruhn KW, Mak PA, Pei L, Hogenesch J, O'Connell R M, Cheng G, Saez E, Miller JF, Tontonoz P. 2004. LXR-dependent gene expression is important for macrophage survival and the innate immune response. *Cell* 119: 299-309
13. Joseph SB, Castrillo A, Laffitte BA, Mangelsdorf DJ, Tontonoz P. 2003. Reciprocal regulation of inflammation and lipid metabolism by liver X receptors. *Nat Med* 9: 213-9
14. Matalonga J, Glaria E, Bresque M, Escande C, Carbo JM, Kiefer K, Vicente R, Leon TE, Beceiro S, Pascual-Garcia M, Serret J, Sanjurjo L, Moron-Ros S, Riera A, Paytubi S, Juarez A, Sotillo F, Lindbom L, Caelles C, Sarrias MR, Sancho J, Castrillo A, Chini EN, Valledor AF. 2017. The Nuclear Receptor LXR Limits Bacterial Infection of Host Macrophages through a Mechanism that Impacts Cellular NAD Metabolism. *Cell Rep* 18: 1241-55
15. Ito A, Hong C, Rong X, Zhu X, Tarling EJ, Hedde PN, Gratton E, Parks J, Tontonoz P. 2015. LXRs link metabolism to inflammation through Abca1-

dependent regulation of membrane composition and TLR signaling. *Elife* 4: e08009

16. Kidani Y, Bensinger SJ. 2012. Liver X receptor and peroxisome proliferator-activated receptor as integrators of lipid homeostasis and immunity. *Immunol Rev* 249: 72-83

17. Miller JC, Brown BD, Shay T, Gautier EL, Jojic V, Cohain A, Pandey G, Leboeuf M, Elpek KG, Helft J, Hashimoto D, Chow A, Price J, Greter M, Bogunovic M, Bellemare-Pelletier A, Frenette PS, Randolph GJ, Turley SJ, Merad M. 2012. Deciphering the transcriptional network of the dendritic cell lineage. *Nat Immunol* 13: 888-99

18. Zhong L, Yang Q, Xie W, Zhou J. 2014. Liver X receptor regulates mouse GM-CSF-derived dendritic cell differentiation in vitro. *Mol Immunol* 60: 32-43

19. Geyeregger R, Zeyda M, Bauer W, Kriehuber E, Saemann MD, Zlabinger GJ, Maurer D, Stulnig TM. 2007. Liver X receptors regulate dendritic cell phenotype and function through blocked induction of the actin-bundling protein fascin. *Blood* 109: 4288-95

20. Torocsik D, Barath M, Benko S, Szeles L, Dezso B, Poliska S, Hegyi Z, Homolya L, Szatmari I, Lanyi A, Nagy L. 2010. Activation of liver X receptor sensitizes human dendritic cells to inflammatory stimuli. *J Immunol* 184: 5456-65

21. Kiss M, Czimmerer Z, Nagy L. 2013. The role of lipid-activated nuclear receptors in shaping macrophage and dendritic cell function: From physiology to pathology. *J Allergy Clin Immunol* 132: 264-86

22. Hamilton JA AA. 2013. Colony stimulating factors and myeloid cell biology in health and disease. *Trends Immunol.* 34 81-9.

23. Partida-Sanchez S, Cockayne DA, Monard S, Jacobson EL, Oppenheimer N, Garvy B, Kusser K, Goodrich S, Howard M, Harmsen A, Randall TD, Lund FE. 2001. Cyclic ADP-ribose production by CD38 regulates intracellular calcium release, extracellular calcium influx and chemotaxis in neutrophils and is required for bacterial clearance in vivo. *Nat Med* 7: 1209-16

24. Lischke T, Heesch K, Schumacher V, Schneider M, Haag F, Koch-Nolte F, Mittrucker HW. 2013. CD38 controls the innate immune response against Listeria monocytogenes. *Infect Immun* 81: 4091-9

25. Vecchi A, Massimiliano L, Ramponi S, Luini W, Bernasconi S, Bonecchi R, Allavena P, Parmentier M, Mantovani A, Sozzani S. 1999. Differential responsiveness to constitutive vs. inducible chemokines of immature and mature mouse dendritic cells. *J Leukoc Biol* 66: 489-94

26. Randolph GJ OJ, Partida-Sánchez S. 2008. Migration of dendritic cell subsets and their precursors. *Annu Rev Immunol.* 26: 293-316.

27. Randolph GJ, Ochando J, Partida-Sanchez S. 2008. Migration of dendritic cell subsets and their precursors. *Annu Rev Immunol* 26: 293-316

28. Escribano C, Delgado-Martin C, Rodriguez-Fernandez JL. 2009. CCR7-dependent stimulation of survival in dendritic cells involves inhibition of GSK3beta. *J Immunol* 183: 6282-95

29. Sánchez-Sánchez N R-BL, Rodríguez-Fernández JL. 2006. The multiple personalities of the chemokine receptor CCR7 in dendritic cells. *J Immunol.* 176: 5153-9.

30. Kellermann SA, Hudak S, Oldham ER, Liu YJ, McEvoy LM. 1999. The CC chemokine receptor-7 ligands 6Ckine and macrophage inflammatory protein-3 beta are potent chemoattractants for in vitro- and in vivo-derived dendritic cells. *J Immunol* 162: 3859-64
31. Foxman EF, Campbell JJ, Butcher EC. 1997. Multistep navigation and the combinatorial control of leukocyte chemotaxis. *J Cell Biol* 139: 1349-60
32. Lund FE. 2006. Signaling properties of CD38 in the mouse immune system: enzyme-dependent and -independent roles in immunity. *Mol Med* 12: 328-33
33. Partida-Sanchez S GA, Fliegert R, Siebrands CC, Dammermann W, Shi G,, Mousseau BJ S-TA, Bhagat H, Walseth TF, Guse AH, Lund FE. 2007. Chemotaxis of mouse bone marrow neutrophils and dendritic cells is controlled by adp-ribose, the major product generated by the CD38 enzyme reaction. *J Immunol.* 179:7827-39.
34. Lee SD, Tontonoz P. 2015. Liver X receptors at the intersection of lipid metabolism and atherogenesis. *Atherosclerosis* 242: 29-36
35. A-Gonzalez N, Guillen JA, Gallardo G, Diaz M, de la Rosa JV, Hernandez IH, Casanova-Acebes M, Lopez F, Tabraue C, Beceiro S, Hong C, Lara PC, Andujar M, Arai S, Miyazaki T, Li S, Corbi AL, Tontonoz P, Hidalgo A, Castrillo A. 2013. The nuclear receptor LXRalpha controls the functional specialization of splenic macrophages. *Nat Immunol* 14: 831-9
36. Bensinger SJ, Bradley MN, Joseph SB, Zelcer N, Janssen EM, Hausner MA, Shih R, Parks JS, Edwards PA, Jamieson BD, Tontonoz P. 2008 LXR signaling couples sterol metabolism to proliferation in the acquired immune response. *Cell.* 134: 97-111.
37. A-Gonzalez N, Bensinger SJ, Hong C, Beceiro S, Bradley MN, Zelcer N, Deniz J, Ramirez C, Diaz M, Gallardo G, de Galarreta CR, Salazar J, Lopez F, Edwards P, Parks J, Andujar M, Tontonoz P, Castrillo A. 2009. Apoptotic cells promote their own clearance and immune tolerance through activation of the nuclear receptor LXR. *Immunity* 31: 245-58
38. Feig JE, Pineda-Torra I, Sanson M, Bradley MN, Vengrenyuk Y, Bogunovic D, Gautier EL, Rubinstein D, Hong C, Liu J, Wu C, van Rooijen N, Bhardwaj N, Garabedian M, Tontonoz P, Fisher EA. 2010. LXR promotes the maximal egress of monocyte-derived cells from mouse aortic plaques during atherosclerosis regression. *J Clin Invest* 120: 4415-24
39. Villablanca EJ, Raccosta L, Zhou D, Fontana R, Maggioni D, Negro A, Sanvito F, Ponzoni M, Valentinis B, Bregni M, Prinetti A, Steffensen KR, Sonnino S, Gustafsson JA, Doglioni C, Bordignon C, Traversari C, Russo V. 2009. Tumor-mediated liver X receptor-alpha activation inhibits CC chemokine receptor-7 expression on dendritic cells and dampens antitumor responses. *Nat Med* 16: 98-105
40. Bruckner M, Dickel D, Singer E, Legler DF. 2012. Converse regulation of CCR7-driven human dendritic cell migration by prostaglandin E(2) and liver X receptor activation. *Eur J Immunol* 42: 2949-58
41. Wu C, Hussein MA, Shrestha E, Leone S, Aiyegbo MS, Lambert WM, Pourcet B, Cardozo T, Gustafson JA, Fisher EA, Pineda-Torra I, Garabedian MJ. 2015.

Modulation of Macrophage Gene Expression via Liver X Receptor alpha Serine 198 Phosphorylation. *Mol Cell Biol* 35: 2024-34
42. Valledor AF, Hsu LC, Ogawa S, Sawka-Verhelle D, Karin M, Glass CK. 2004. Activation of liver X receptors and retinoid X receptors prevents bacterial-induced macrophage apoptosis. *Proc Natl Acad Sci U S A* 101: 17813-8
43. Frasca L, Fedele G, Deaglio S, Capuano C, Palazzo R, Vaisitti T, Malavasi F, Ausiello CM. 2006. CD38 orchestrates migration, survival, and Th1 immune response of human mature dendritic cells. *Blood* 107: 2392-9
44. Malavasi F, Deaglio S, Ferrero E, Funaro A, Sancho J, Ausiello CM, Ortolan E, Vaisitti T, Zubiaur M, Fedele G, Aydin S, Tibaldi EV, Durelli I, Lusso R, Cozno F, Horenstein AL. 2006. CD38 and CD157 as receptors of the immune system: a bridge between innate and adaptive immunity. *Mol Med* 12: 334-41
45. Zubiaur M, Fernandez O, Ferrero E, Salmeron J, Malissen B, Malavasi F, Sancho J. 2002. CD38 is associated with lipid rafts and upon receptor stimulation leads to Akt/protein kinase B and Erk activation in the absence of the CD3-zeta immune receptor tyrosine-based activation motifs. *J Biol Chem* 277: 13-22
46. Glass CK, Witztum JL. 2001. Atherosclerosis. the road ahead. *Cell* 104: 503-16
47. Cybulsky MI, Cheong C, Robbins CS. 2016. Macrophages and Dendritic Cells: Partners in Atherogenesis. *Circ Res* 118: 637-52
48. Fisher EA. 2016. Regression of Atherosclerosis: The Journey From the Liver to the Plaque and Back. *Arterioscler Thromb Vasc Biol* 36: 226-35
49. Luchtefeld M, Grothusen C, Gagalick A, Jagavelu K, Schuett H, Tietge UJ, Pabst O, Grote K, Drexler H, Forster R, Schieffer B. 2010. Chemokine receptor 7 knockout attenuates atherosclerotic plaque development. *Circulation* 122: 1621-8
50. Halvorsen B, Dahl TB, Smedbakken LM, Singh A, Michelsen AE, Skjelland M, Krohg-Sorensen K, Russell D, Hopken UE, Lipp M, Damas JK, Holm S, Yndestad A, Biessen EA, Aukrust P. 2014. Increased levels of CCR7 ligands in carotid atherosclerosis: different effects in macrophages and smooth muscle cells. *Cardiovasc Res* 102: 148-56
51. Peet DJ, Turley SD, Ma W, Janowski BA, Lobaccaro JM, Hammer RE, Mangelsdorf DJ. 1998. Cholesterol and bile acid metabolism are impaired in mice lacking the nuclear oxysterol receptor LXR alpha. *Cell* 93: 693-704.
52. Leon B, Ardavin C. 2008. Monocyte migration to inflamed skin and lymph nodes is differentially controlled by L-selectin and PSGL-1. *Blood* 111: 3126-30
53. Inaba K, Inaba M, Romani N, Aya H, Deguchi M, Ikehara S, Muramatsu S, Steinman RM. 1992. Generation of large numbers of dendritic cells from mouse bone marrow cultures supplemented with granulocyte/macrophage colony-stimulating factor. *J Exp Med* 176: 1693-702
54. Thomas WR, Edwards AJ, Watkins MC, Asherson GL. 1980. Distribution of immunogenic cells after painting with the contact sensitizers fluorescein isothiocyanate and oxazolone. Different sensitizers form immunogenic complexes with different cell populations. *Immunology* 39: 21-7

55. Gomez-Cabanas L, Delgado-Martin C, Lopez-Cotarelo P, Escribano-Diaz C, Alonso CL, Riol-Blanco L, Rodriguez-Fernandez JL. 2014. Detecting apoptosis of leukocytes in mouse lymph nodes. *Nat Protoc* 9: 1102-12
56. Tangirala RK, Bischoff ED, Joseph SB, Wagner BL, Walczak R, Laffitte BA, Daige CL, Thomas D, Heyman RA, Mangelsdorf DJ, Wang X, Lusis AJ, Tontonoz P, Schulman IG. 2002. Identification of macrophage liver X receptors as inhibitors of atherosclerosis. *Proc Natl Acad Sci U S A* 99: 11896-901
57. Bradley MN, Hong C, Chen M, Joseph SB, Wilpitz DC, Wang X, Lusis AJ, Collins A, Hseuh WA, Collins JL, Tangirala RK, Tontonoz P. 2007. Ligand activation of LXR beta reverses atherosclerosis and cellular cholesterol overload in mice lacking LXR alpha and apoE. *J Clin Invest* 117: 2337-46
58. Tangirala RK, Tsukamoto K, Chun SH, Usher D, Pure E, Rader DJ. 1999. Regression of atherosclerosis induced by liver-directed gene transfer of apolipoprotein A-I in mice. *Circulation* 100: 1816-22
59. Zelcer N, Khanlou N, Clare R, Jiang Q, Reed-Geaghan EG, Landreth GE, Vinters HV, Tontonoz P. 2007 Attenuation of neuroinflammation and Alzheimer's disease pathology by liver x receptors. *Proc Natl Acad Sci U S A.* 104: 10601-6.
60. Joseph SB, McKilligin E, Pei L, Watson MA, Collins AR, Laffitte BA, Chen M, Noh G, Goodman J, Hagger GN, Tran J, Tippin TK, Wang X, Lusis AJ, Hsueh WA, Law RE, Collins JL, Willson TM, Tontonoz P. 2002. Synthetic LXR ligand inhibits the development of atherosclerosis in mice. *Proc Natl Acad Sci U S A* 99: 7604-9

FIGURE LEGENDS

Figure 1. Transcription factor and nuclear receptor expression profiles in ex vivo differentiated mouse and human DCs. (A) Expression of transcription factors including nuclear receptors in mouse BMDCs (left panel) and human monocyte-derived DCs (right panel) were compared to all probe sets of Affymetrix microarray. If more than one probe sets represent a certain gene, the probe set having the highest signal intensity is shown. (B) Microarray-based comparison of the number of highly, moderately and not expressed transcription factors as well as nuclear receptors in mouse and human ex vivo differentiated DCs. (C) Heatmap illustrating differentially or commonly nuclear receptors expression in different types of human and mouse DCs. Blue indicates low expression and red indicates high expression levels. We identified both LXRα and LXRβ in a selected list of that are moderately to highly expressed.

Figure 2. Differentiation and activation of DCs from WT and LXR-DKO mice. WT and LXR-DKO MoDCs were differentiated *in vitro* (A-B). (A) Flow cytometry analysis of MHC-II and CD11c expression (B) Flow cytometry analysis of the expression of DC maturation markers MHC-II, CD80, CD86 and CD69. Mean fluorescence intensity quantifications are graphed below each plot. (C) Left panel: Flow cytometry analysis of classic MHC-II+/CD11c+ DCs in splenic and LN cell suspensions from WT and LXR-DKO mice. Right panel: Immunofluorescence analysis of spleen and LN sections from WT and LXR-DKO mice showing combinations of double stainings with antibodies that recognize CD11c+ DCs and CD4+/CD8+ cells within the T-cell zone (spleen) or CD11c+ DCs and CD169+ subcapsular sinus macrophages (LN). Scale bars represent 100μm or 50μm in spleen and LN samples respectively. (D): Immunofluorescence analysis of MHC-II and CD68 expression in epidermal sheets prepared from WT and LXR-DKO mice. (A-D) Representative plots and images are shown from two independent experiments with *n*=3-4 mice per genotype.

Figure 3: Influence of LXR deficiency during DC maturation. Influence of LXR deficiency during DC maturation. (A) Real-time qPCR analysis of Abca1 and Pltp gene expression in WT iDCs and mDCs in response to LXR synthetic ligand GW3965 (1 uM, 24 hours). Statistical analysis was performed via Student's t test. *p< 0.05. Error bars represent mean ±SD. (B) LXR target gene expression during DC maturation (mDCs vs iDCs, 24 hours LPS, 100ng/mL) and in response to GW3965 (1 μM, 24 hours) in mDCs. (C) Transcriptional profiling of iDCs and mDCs WT and LXR-DKO. Left panel: Venn Diagram representation showing the overlap of upregulated genes (5 fold or more in mDC vs iDC) in WT and LXR-DKO DCs. Middle panel: Heatmap illustrating differentially or commonly regulated genes in WT and LXR-DKO mDCs vs iDCs. Right panel: top KEGG pathways obtained from GO analysis of the exclusive or common-induced genes in WT and LXR-DKO DCs during DC maturation. Examples of representative genes from each group are listed.

Figure 4: *Cd38* as an LXR-responsive gene in DCs. A) mRNA expression of Abca1, Cd38, Srebf1, Abcg1 and in WT and LXR-DKO iDCs and mDCs. (B) Regulation of mRNA expression of Srebf1 and Cd38 in WT and LXR-DKO iDCs and mDCs in response to GW3965 (1 um, 24 hours). (A-B) Error bars represent mean ± SD. *p < 0.05, **p < 0.01 and †p < 0.05 (C) Immunofluorescence microscopy analysis of CD38 protein expression in WT and LXR-DKO mDCs in the presence of LXR agonist GW3965 (LPS 100ng/ml for maturation and 1uM GW3965 added simultaneously). (D) Flow cytometry analysis of CD38 protein expression in WT and LXR-DKO iDCs and mDCs compared to isotype control antibody. (C-D) Representative images and plots obtained from three independent experiments.

Figure 5. mRNA expression of Cd38 and established LXR targets was analyzed by real-time qPCR in human monocyte-derived iDCs and mDCs. Cells were obtained from CD14+ monocytes isolated from buffy coats, differentiated 7 days with GMCSF+IL-4 and further stimulated 24 hours with LPS in the absence or presence of 1 □M of GW3965. Representative graphs from 3 independent

experiments. Error bars represent mean ± SD of three experiments $**p < 0.01$ and $*p < 0.05$.

Figure 6: Deficient chemotactic response in LXR-DKO DCs in response to CCL19/CCL21.

(A) Chemotaxis of WT and LXR-DKO iDCs and mDCs was analyzed in transwell migration assays in response to CCL19 and CCL21 (100ng/mL, 3 hours). (B) Chemotaxis of isolated splenic DCs from WT and LXR-DKO was analyzed in response to CCL19 and CCL21 and GW3965. (C) Activation of signaling pathways by CCL19 in WT and LXR-DKO BM-derived mDCs. Cells were treated CCL19 for the indicated times and protein extracts were analyzed by western blot with antibodies that recognize phospho-ERK, ERK1/2, phospho-AKT and β-actin. Western blot is representative of 3 independent experiments. (A-B) Graphs and are representative from 3 independent experiments with triplicate samples. *p < 0.05

Figure 7: Impaired migration of LXR-DKO DCs *in vivo*

(A) Skin contact sensitizer-induced DC migration to draining LNs. FITC+ DCs were identified by immunofluorescence analysis of consecutive sections of WT and LXR-DKO LNs isolated 24-48 hours after FITC-painting. CD11c+/FITC+ DCs were localized within the T-cell zone (CD3+). Graph below represents the frequency of CD11c+/FITC+ DCs analyzed by flow cytometry of LN cell suspensions obtained from mice painted with FITC for 24 and 48h (bottom panel). (B) $2x10^6$ WT and LXR-DKO BMDCs were labelled with CellTracker red and green respectively and co-injected into footpads of WT mice. Inguinal LNs were isolated after 24h post-injection; tissue and cell suspensions were analyzed by immunofluorescence microscopy and flow cytometry. Immunofluorescence microscopy results are representative of three independent experiments with n=3 mice. Graphs represent mean ± SD of three experiments. **p<0.01 and *p < 0.05.

Figure 8: CD38 activity is required for LXR-dependent regulation of DC chemotaxis.

(A) Analysis of in vitro transwell migration of WT and LXRDKO mDCs in the presence of a CD38 inhibitor. (B) Genetic absence of CD38 abolished LXR-dependent DC chemotaxis. Chemotaxis of WT, CD38-KO and LXR-DKO mDCs was analyzed in transwell migration assays in response to CCL19 and GW3965. Error bars represent mean ± SD.$**p < 0.01$ and $*p < 0.05$.

Figure 9: (A) Analysis of blood leukocyte populations obtained from WT and CD38-/- mice under homeostatic conditions (N=5 each group). (B) Lethally irradiated C57BL/6 CD45.1+ hosts were reconstituted with either C57BL/6 CD45.2+ or CD38KO CD45.2 donor cells. Twelve weeks post-reconstitution peripheral blood myeloid and lymphoid populations were analyzed by flow cytometry. (C) Analysis of host/donor percentage of CD11c+ cells in spleen, bone marrow and skin of WT or CD38-/- transplanted mice. Virtually all bone marrow and spleen tissues contain cells of donor origin, whereas the majority of cells in the skin are host-derived. (D) The skin of reconstituted mice was sensitized with DNFB in acetone and 3 or 6 days post-sensitization, analysis of local skin LC emigration and bone marrow–derived skin LC renewal, in both groups by enumerating CD11c+ cells in inflamed skin from host and donor origin.

Figure 10: CD38 expression in bone-marrow cells is important for atherosclerosis development: (A) Percentage of aorta surface area with atherosclerotic plaque in transplanted LDLR−/− after 18 weeks on a Western diet. Horizontal lines indicate mean ± SEM. Right panel shows representative photographs from en face analysis. N=15-20 mice in each group were analyzed. (B) Representative micrographs of frozen sections from the aortic roots of WT and CD38-/- transplanted mice that were stained with CD68 antibody (N=20 for WT and N=15 for CD38-/-) (C) Quantification of total CD68 signal within atherosclerotic lesions from each group (N=20 for WT and N=15 for CD38-/-). (D) Quantification of CD68 signal relative to each atherosclerotic lesions from both WT and CD38-/- transplanted mice (N=7 per group).

Table 1: Microarray-based comparison of all nuclear receptors expressed in mouse and human ex vivo differentiated DCs.

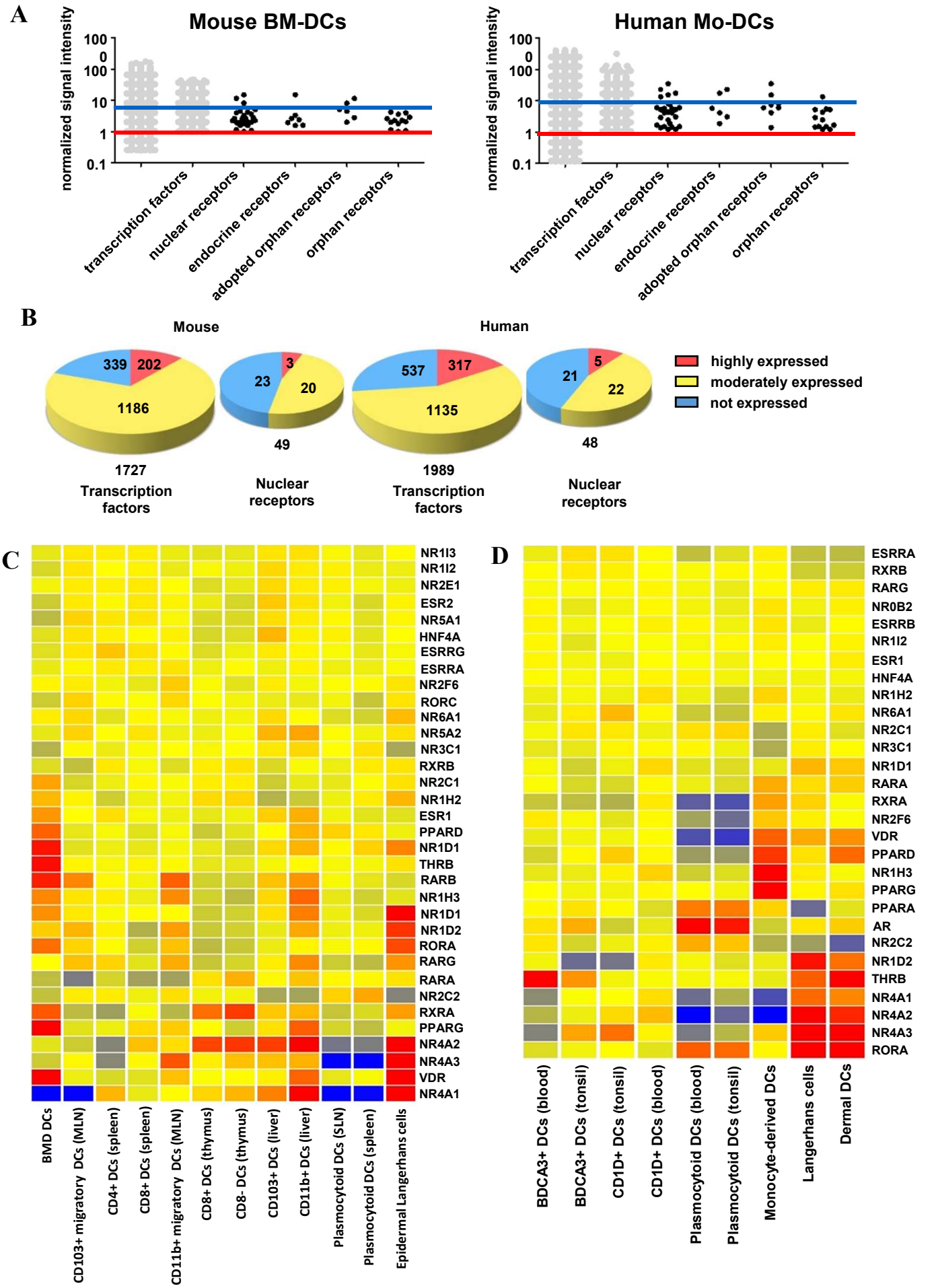

Figure 1: (A) Expression of transcription factors including nuclear receptors in mouse BMDCs (left panel) and human monocyte-derived DCs (right panel) were compared to all probe sets of Affymetrix microarray. If more than one probe sets represent a certain gene, the probe set having the highest signal intensity is shown. (B) Microarray-based comparison of the number of highly, moderately and not expressed transcription factors as well as nuclear receptors in mouse and human ex vivo differentiated DCs. (C) Heatmap illustrating differentially or commonly nuclear receptors expression in different types of human and mouse DCs. Blue indicates low expression and red indicates high expression levels. We identified both LXRα and LXRβ in a selected list of that are moderately to highly expressed.

Endocrine Receptors		Adopted Orphan Receptors		Orphan Receptors	
HUMAN	**MOUSE**	**HUMAN**	**MOUSE**	**HUMAN**	**MOUSE**
Highly expressed nuclear receptors					
NR1I1-VDR NR3C1-GR	NR1I1-VDR	NR2B1-Rxrα NR1C2-Pparδ	NR1C3-Pparγ NR1H2-Lxrβ	NR4A3-Nor1	
Moderately expressed nuclear receptors					
NR1B1-Rarα NR1B3-Rarγ NR3A1-Erα NR1A1-Trα	NR1A1-Trα NR3C1-GR NR1B2-Rarβ NR1A2-Trβ NR1B1-Rarα NR3A1-Erα NR1B3-Rarγ	NR1C3-Pparγ NR1H3-Lxrα NR1H2-Lxrβ NR2B2-Rxrβ NR1C1-Pparα NR1I2-Pxr	NR1C2-Pparδ NR2B1-Rxrα NR2B2-Rxrβ NR1H3-Lxrα	NR2F6-Ear2 NR3B1-Errα NR1D1-Rev-Erbα NR2C2-Tr4 NR1F3-Rorγ NR4A1-NgfiB NR0B2-Shp NR2A1-Hnf4α NR3B2-Errβ NR2C1-Tr2 NR2F1-Coup-TFI NR6A1-Gcnf	NR2C2-Tr4 NR4A3-Nor1 NR2C1-Tr2 NR1D2-Rev-Erbβ NR3B1-Errα NR1F1-Rorα NR1D1-Rev-Erbα NR4A2-Nurr1 NR2F6-Ear2 NR6A1-Gcnf NR2A1-Hnf4α NR4A1-NgfiB

Table 1: Microarray-based comparison of all nuclear receptors expressed in mouse and human ex vivo differentiated DCs.

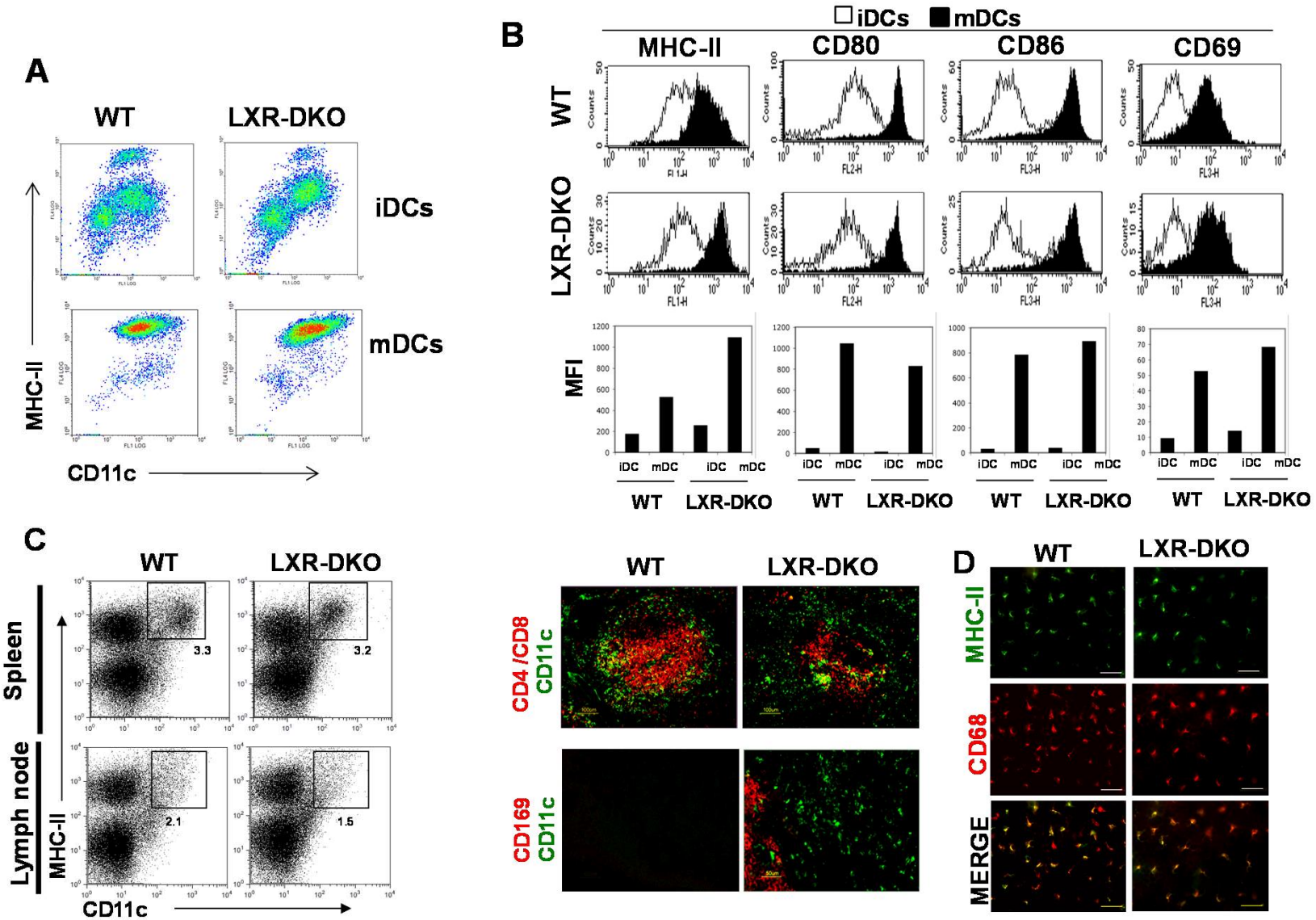

Figure 2: Differentiation and activation of DCs from WT and LXR-DKO mice. WT and LXR-DKO MoDCs were differentiated in vitro (A-B). Flow cytometry analysis of MHC-II and CD11c expression (A) and DC maturation markers MHC-II, CD80, CD86 and CD69 (B). Mean fluorescence intensity quantifications are graphed below each plot. (C) Left panel: Flow cytometry analysis of classic MHC-II+/CD11c+ DCs in splenic and LN cell suspensions from WT and LXR-DKO mice. Right panel: Immunofluorescence analysis of spleen and LN sections from WT and LXR-DKO mice showing combinations of double stainings with antibodies that recognize CD11c+ DCs and CD4+/CD8+ cells within the T-cell zone (spleen) or CD11c+ DCs and CD169+ subcapsular sinus macrophages (LN). Scale bars represent 100µm or 50µm in spleen and LN samples respectively. (D): Immunofluorescence analysis of MHC-II and CD68 expression in epidermal sheets prepared from WT and LXR-DKO mice. (A-D) Representative plots and images are shown from two independent experiments with n=3-4 mice per genotype.

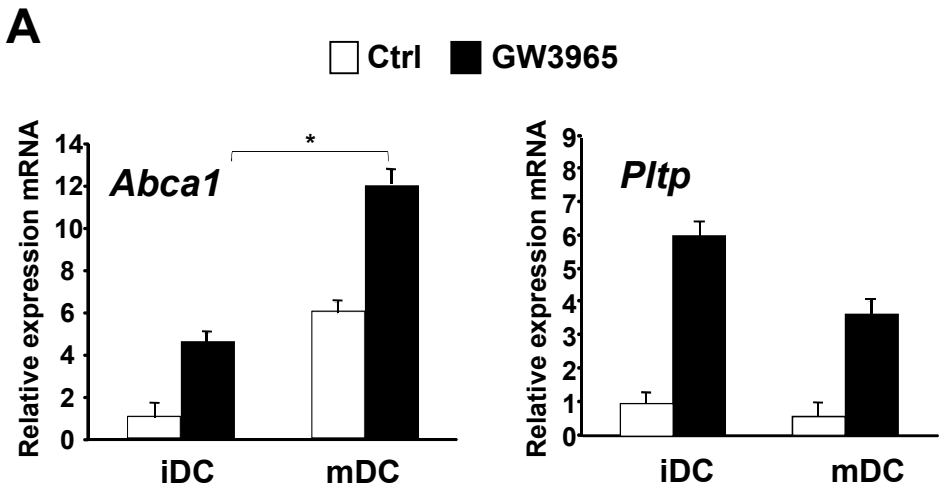

B

Gene	Average induction mature DC	Average induction by GW3965
ABCA1	7.5	3,5
ApoC2	2.0	3.0
PLTP	0.80	3,2
ApoE	0.75	3.5
SREBP1c	0.60	3.9
LPL	0.60	2.4
ABCG1	0.60	3.2
SCD1	0.55	2.2

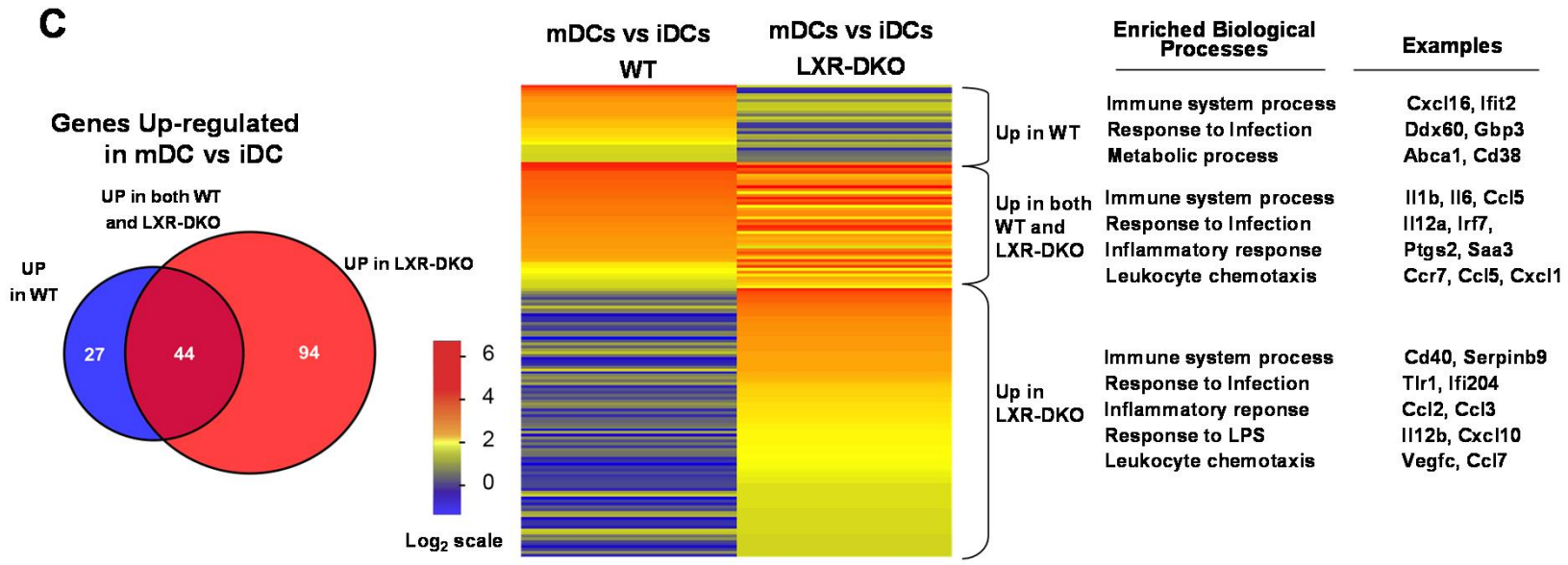

Figure 3: Influence of LXR deficiency during DC maturation. (A) Real-time qPCR analysis of Abca1 and Pltp gene expression in WT iDCs and mDCs in response to LXR synthetic ligand GW3965 (1 uM, 24 hours). Statistical analysis was performed via Student's t test. *p< 0.05. Error bars represent mean ±SD. (B) LXR target gene expression during DC maturation (mDCs vs iDCs, 24 hours LPS, 100ng/mL) and in response to GW3965 (1 µM, 24 hours) in mDCs. (C) Transcriptional profiling of iDCs and mDCs WT and LXR-DKO. Left panel: Venn Diagram representation showing the overlap of upregulated genes (5 fold or more in mDC vs iDC) in WT and LXR-DKO DCs. Middle panel: Heatmap illustrating differentially or commonly regulated genes in WT and LXR-DKO mDCs vs iDCs. Right panel: top KEGG pathways obtained from GO analysis of the exclusive or common-induced genes in WT and LXR-DKO DCs during DC maturation. Examples of representative genes from each group are listed.

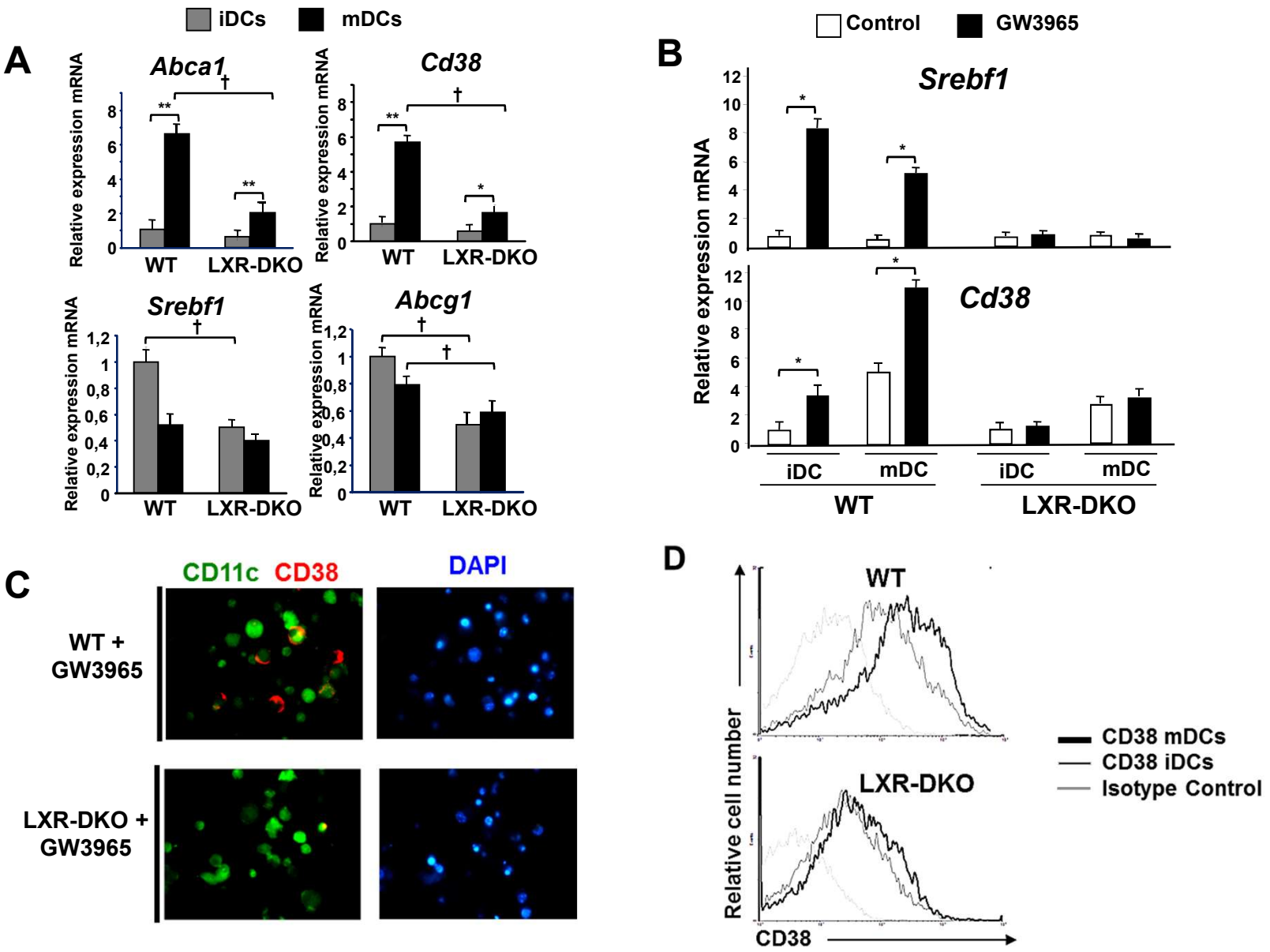

Figure 4: A) mRNA expression of Abca1, Cd38, Srebf1, Abcg1 and in WT and LXR-DKO iDCs and mDCs. (B) Regulation of mRNA expression of Srebf1 and Cd38 in WT and LXR-DKO iDCs and mDCs in response to GW3965 (1 um, 24 hours). (A-B) Error bars represent mean ± SD. *p < 0.05, **p < 0.01 and †p < 0.05 (C) Immunofluorescence microscopy analysis of CD38 protein expression in WT and LXR-DKO mDCs in the presence of LXR agonist GW3965 (LPS 100ng/ml for maturation and 1uM GW3965 added simultaneously). (D) Flow cytometry analysis of CD38 protein expression in WT and LXR-DKO iDCs and mDCs compared to isotype control antibody. (C-D) Representative images and plots obtained from three independent experiments.

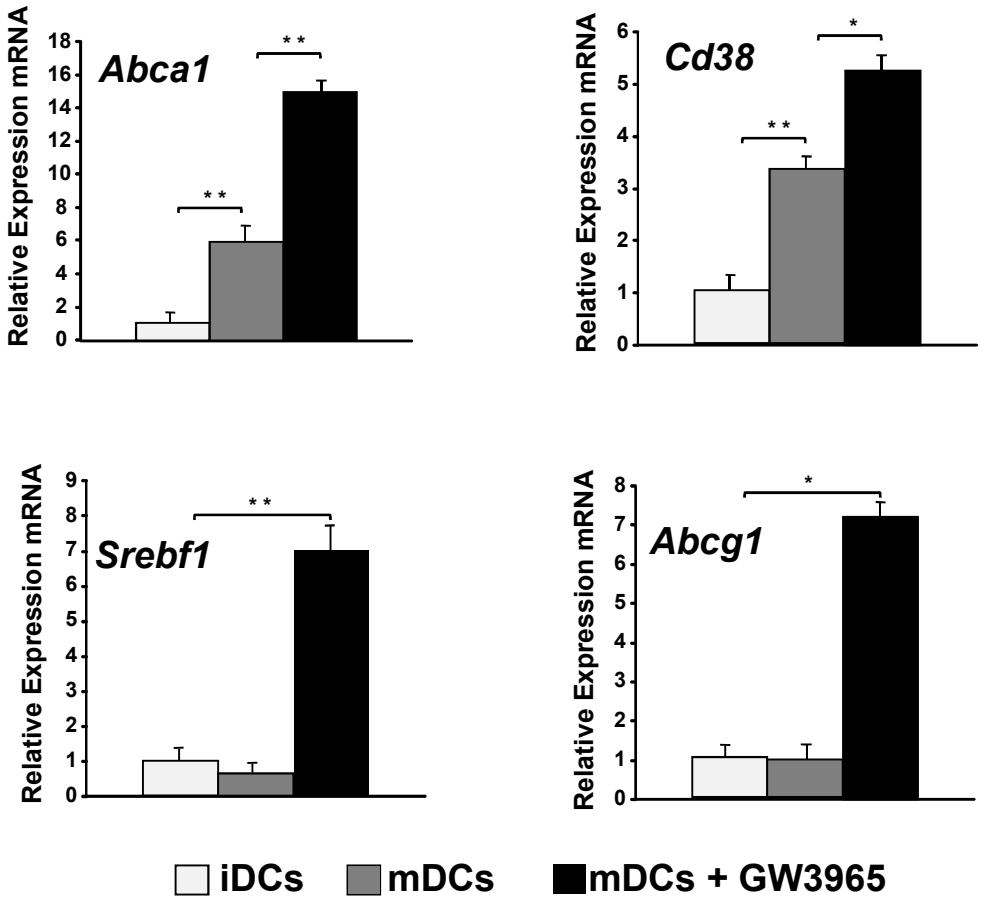

Figure 5. mRNA expression of *Cd38* and established LXR targets was analyzed by real-time qPCR in human monocyte-derived iDCs and mDCs. Cells were obtained from CD14+ monocytes isolated from buffy coats, differentiated 7 days with GMCSF+IL-4 and further stimulated 24 hours with LPS in the absence or presence of 1 μM of GW3965. Representative graphs from 3 independent experiments. Error bars represent mean ± SD of three experiments $^{**}p < 0.01$ and $^{*}p < 0.05$.

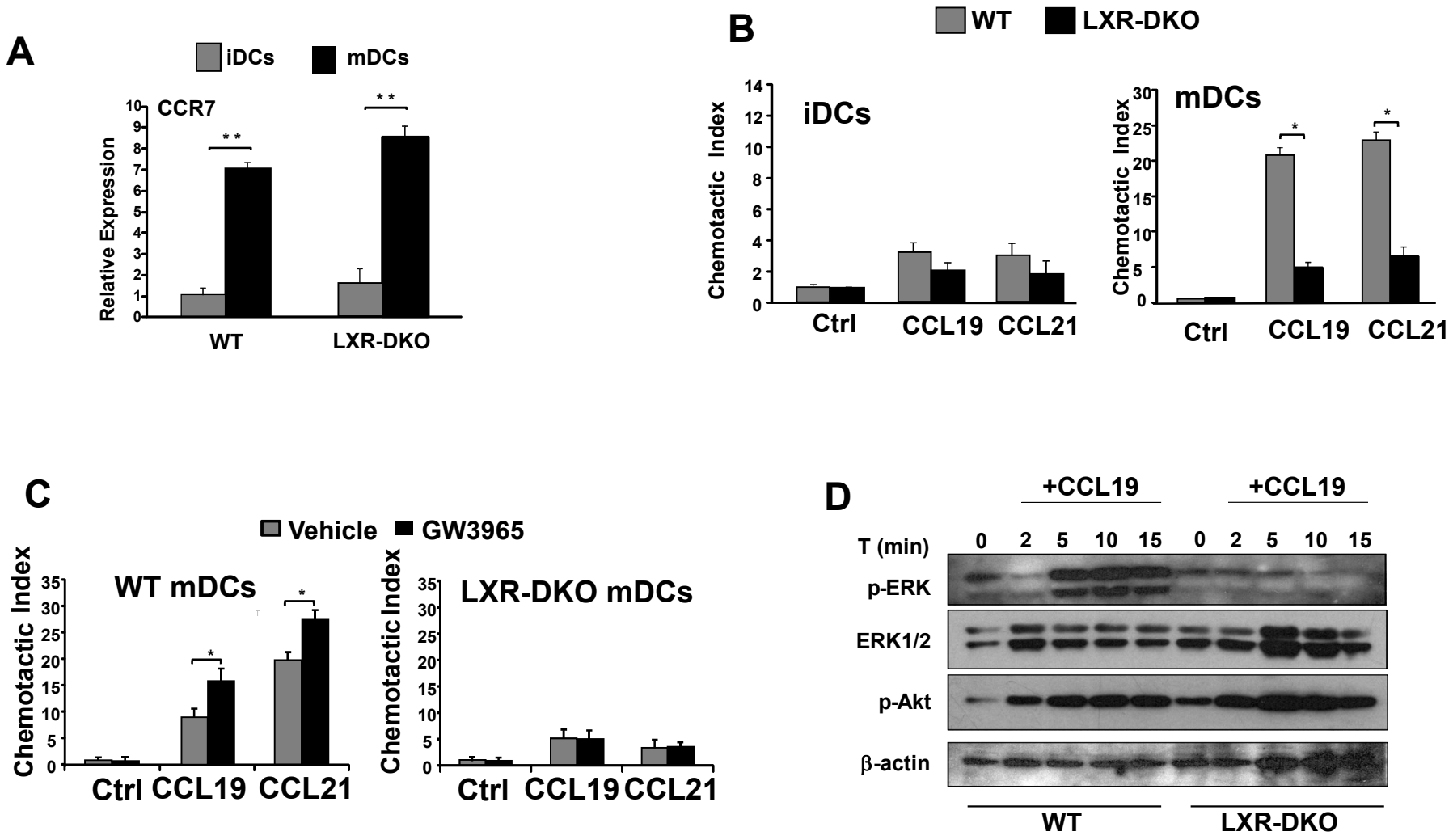

Figure 6: (A) mRNA levels of CCR7 in WT and LXR-DKO iDCs and mDCs analyzed by real-time qPCR. (B) Chemotaxis of WT and LXR-DKO iDCs and mDCs was analyzed in transwell migration assays in response to CCL19 and CCL21 (100ng/mL, 3 hours). (C) Chemotaxis of isolated splenic DCs from WT and LXR-DKO was analyzed in response to CCL19 and CCL21 and GW3965. (D) Activation of signaling pathways by CCL19 in WT and LXR-DKO BM-derived mDCs. Cells were treated CCL19 for the indicated times and protein extracts were analyzed by western blot with antibodies that recognize phospho-ERK, ERK1/2, phospho-AKT and β-actin. Western blot is representative of 3 independent experiments. (A-B) Graphs and are representative from 3 independent experiments with triplicate samples. *$p < 0.05$, **$p < 0.01$.

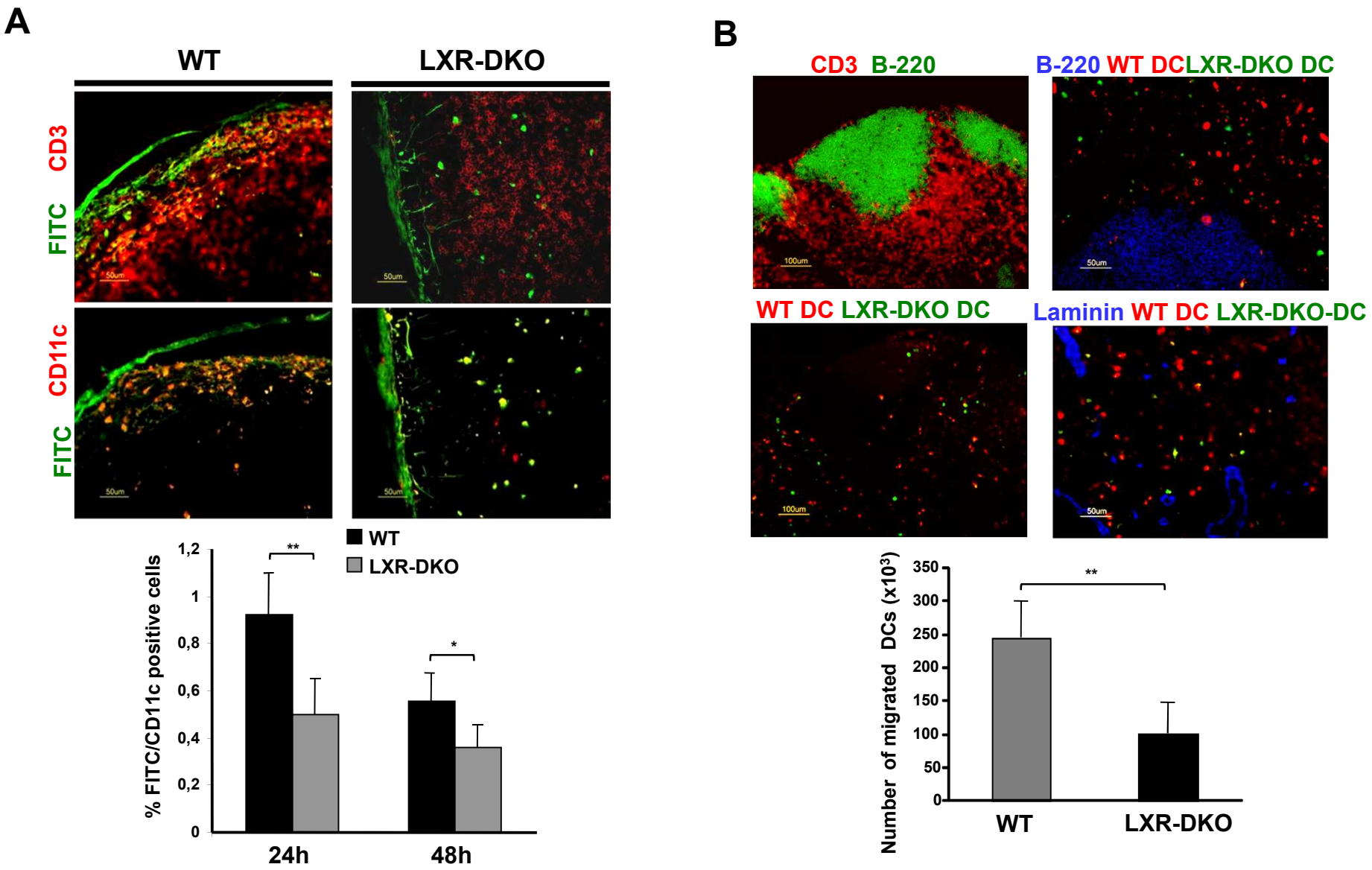

Figure 7: (A) Skin contact sensitizer-induced DC migration to draining LNs. FITC+ DCs were identified by immunofluorescence analysis of consecutive sections of WT and LXR-DKO LNs isolated 24-48 hours after FITC-painting. CD11c+/FITC+ DCs were localized within the T-cell zone (CD3+). Graph below represents the frequency of CD11c+/FITC+ DCs analyzed by flow cytometry of LN cell suspensions obtained from mice painted with FITC for 24 and 48h (bottom panel). (B) 2x106 WT and LXR-DKO BMDCs were labelled with CellTracker red and green respectively and co-injected into footpads of WT mice. Inguinal LNs were isolated after 24h post-injection; tissue and cell suspensions were analyzed by immunofluorescence microscopy and flow cytometry. Immunofluorescence microscopy results are representative of three independent experiments with n=3 mice. Graphs represent mean ± SD of three experiments. **p<0.01 and *p < 0.05.

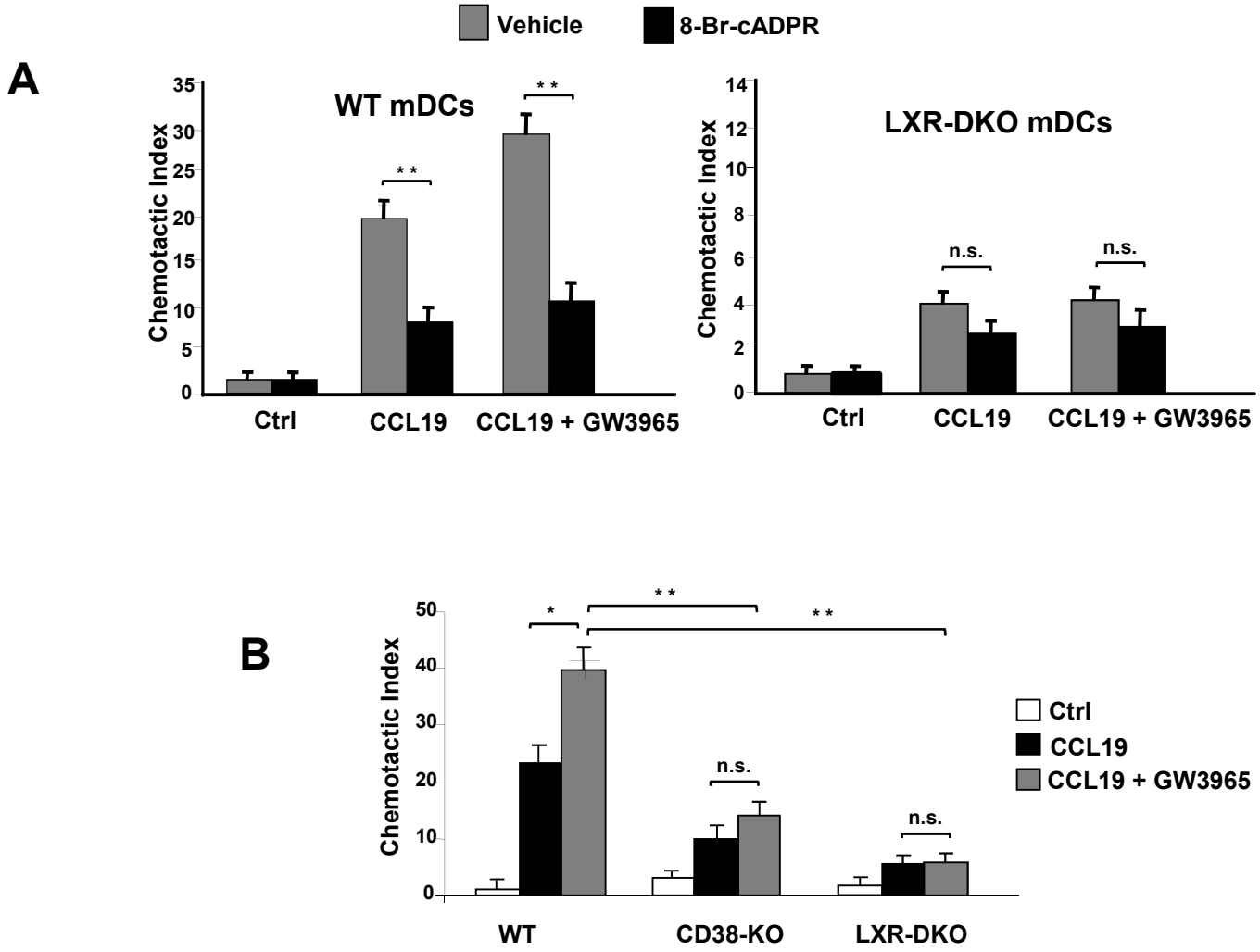

Figure 8: (A) Analysis of in vitro transwell migration of WT and LXRDKO mDCs in the presence of a CD38 inhibitor. (B) Genetic absence of CD38 abolished LXR-dependent DC chemotaxis. Chemotaxis of WT, CD38-KO and LXR-DKO mDCs was analyzed in transwell migration assays in response to CCL19 and GW3965. Error bars represent mean ± SD.$**p < 0.01$ and $*p < 0.05$

A

Blood counts (10^9/L)	WT	CD38-/-	*P*
WBC	2.278 ± 0.54	1.684 ± 0.40	0,4023
Monocytes	0.096 ± 0.01	0.048 ± 0.02	0,0577
Lymphocytes	2.026 ± 0.48	1.454 ± 0.36	0,3678
Granulocytes	0.158 ± 0.05	0.18 ± 0.04	0,752

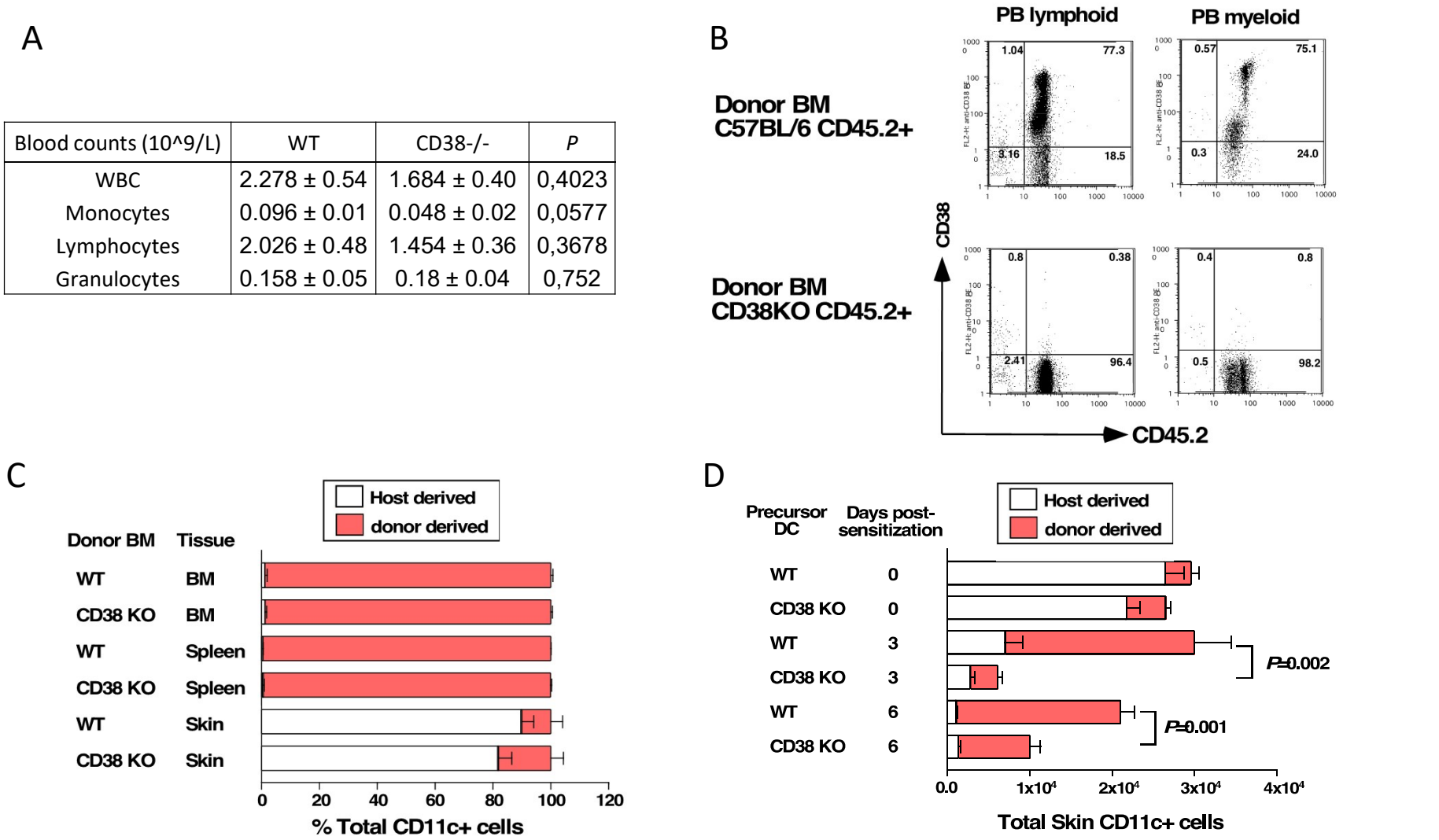

Figure 9 (A) Analysis of blood leukocyte populations obtained from WT and CD38-/- mice under homeostatic conditions (N=5 each group). (B) Lethally irradiated C57BL/6 CD45.1+ hosts were reconstituted with either C57BL/6 CD45.2+ or CD38KO CD45.2 donor cells. Twelve weeks post-reconstitution peripheral blood myeloid and lymphoid populations were analyzed by flow cytometry. (C) Analysis of host/donor percentage of CD11c+ cells in spleen, bone marrow and skin of WT or CD38-/- transplanted mice. Virtually all bone marrow and spleen tissues contain cells of donor origin, whereas the majority of cells in the skin are host-derived. (D) The skin of reconstituted mice was sensitized with DNFB in acetone and 3 or 6 days post-sensitization, analysis of local skin LC emigration and bone marrow–derived skin LC renewal, in both groups by enumerating CD11c+ cells in inflamed skin from host and donor origin.

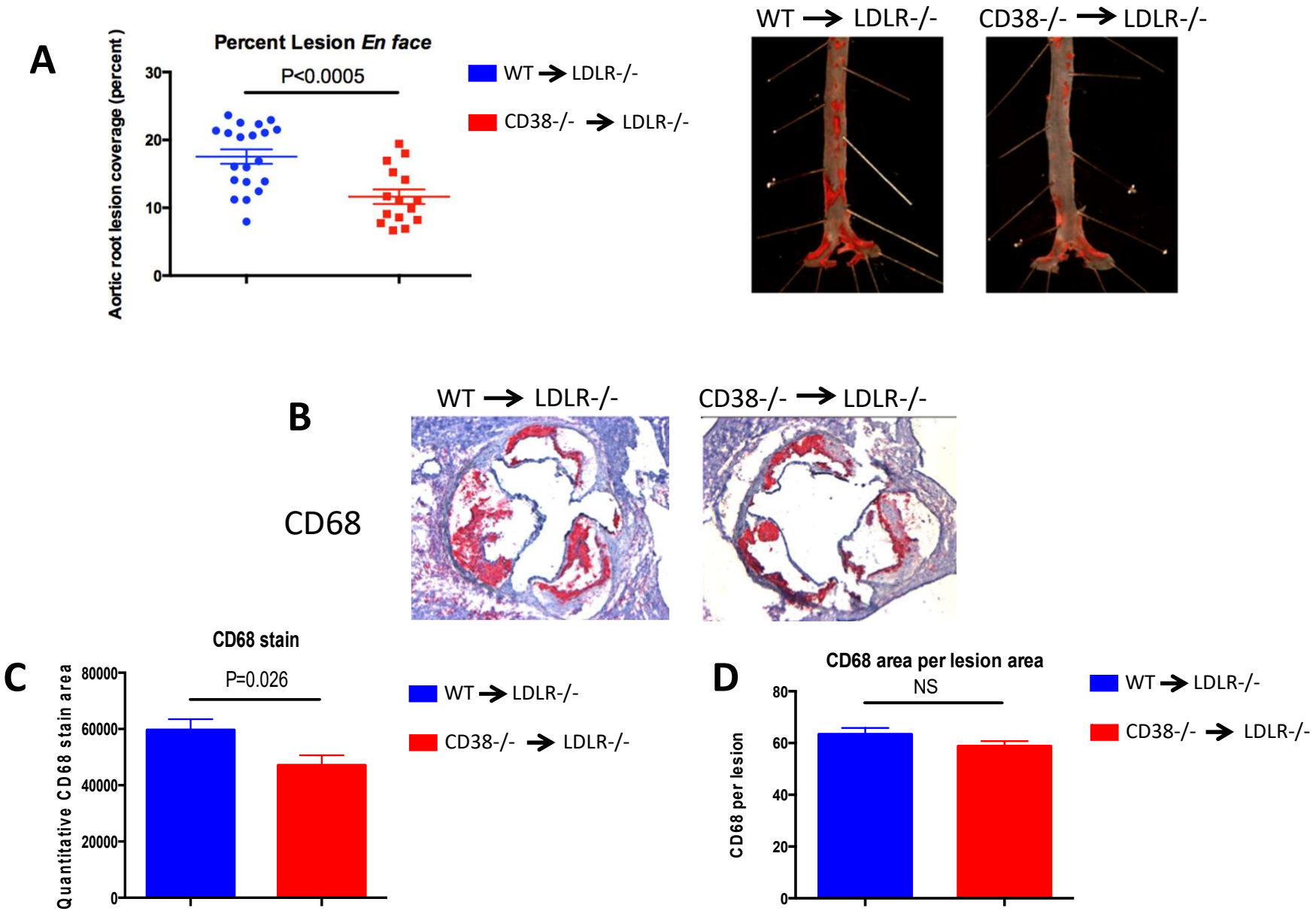

Figure 10: (A) Percentage of aorta surface area with atherosclerotic plaque in transplanted LDLR−/− after 18 weeks on a Western diet. Horizontal lines indicate mean ± SEM. Right panel shows representative photographs from en face analysis. N=15-20 mice in each group were analyzed. (B) Representative micrographs of frozen sections from the aortic roots of WT and CD38-/- transplanted mice that were stained with CD68 antibody (N=20). (C) Quantification of total CD68 signal within atherosclerotic lesions from each group (N=20). (D) Quantification of CD68 signal relative to each atherosclerotic lesions from both WT and CD38-/- transplanted mice (N=7).